Titan's Interaction with the Solar Wind and Saturn's Magnetospheric Plasma

by

Douglas E. Jones

Dept. of Physics and Astronomy,
Brigham Young University
Provo, Utah

Submitted to: ENCYCLIA, The Journal of the Utah Academy of Sciences, Arts and Letters (July, 1984)

Introduction

As a result of a number of factors, the flowing plasma-satellite interaction at Titan is expected to be the most varied of any object in the solar system. This is primarily due to the fact that for a little over half of the time its orbit lies outside Saturn's subsolar magnetopause, exposing it to either the free streaming solar wind, where the interaction is usually described as being both supersonic and superalfvenic, or to the thermalized solar wind or magnetosheath plasma, where the interaction is usually subsonic and superalfvenic. During the remainder of the time, Titan is located within Saturn's magnetosphere and is subsequently exposed to the nearly corotating magnetospheric plasma. The temperature, composition and density of the latter undergoes both temporal and spatial variations and as a result, the interaction can be any combination of the sub/trans/supersonic and sub/trans/superalfvenic possibilities.

In this paper we will review a number of aspects of the interaction of Titan with the solar wind and Saturn's magnetospheric plasma and report the results of a number of relevant studies. We will first consider the likelihood of Titan being exposed to the free streaming solar wind, the shocked solar wind or magnetosheath plasma, and the corotating magnetospheric plasma. We then report the results of calculations of the charge exchange absorption and mass loading of both the solar wind and magnetospheric plasma by two model Titan atmospheres that have been proposed, and discuss the implications of these results in terms of a Titan bow shock and a possible cometary type of interaction. We then discuss the Voyager 1 and Pioneer 11 magnetic field results in terms of Titan's magnetic tail and wake.

Solar Wind Pressure Variations and the Plasma Environment at Titan.

Acuna and Ness (1980) first noted that Titan's orbit (20.2 R_S; R_S = Saturn radius) is near the nominal location of the subsolar magnetopause of Saturn. Wolf and Neubauer (1982) subsequently outlined the variable magnetoplasma conditions that Titan could be exposed to while in it's orbit, considering varying solar wind conditions and the resulting configurations of Saturns magnetosphere. Figure 1 [Slavin et al., (1983)] displays a histogram of the number of hours out of a total of 1275 that Saturn's sub-solar

magnetopause was at any given distance. The mean is observed to be 18.8 R_S, or within Titan's orbit. Hence, when near the noon meridian plane, Titan will be beyond Saturn's magnetopause more than 50% of the time. Using 1.33 as the ratio of the subsolar shock-to-magnetopause distance ratio, a 20.2 R_S shock distance corresponds to a magnetopause distance of 15.2 R_S. Referring to Figure 1, we see that Titan will be at or beyond the shock location about 10% of the time. The solar wind pressure corresponding to Titan at or beyond Saturn's magnetopause is about 2.3 X 10^{-10} dynes/cm^2, and to be beyond the bow shock requires a pressure greater than about 1 X 10^{-9} dynes/cm^2. Inspection of Figure 1 suggests that while in the terminator plane, there is even a small (2 - 3%) chance of Titan being in the supersonic portion of the magnetosheath.

Based upon an earlier estimate of Titan's magnetic moment by Neubauer (1978), the existance of a Mercury-like magnetic field standoff configuration was considered possible because the estimated surface field of 100 nT provided sufficient pressure to hold off a solar wind pressure of 4 X 10^{-9} dynes/cm^2, i.e., such a field would be able to withstand the > 1 X 10^{-9} dyne/cm^2 pressure needed to push the bow shock to within the orbit of Titan. However, using Voyager 1 magnetic field data obtained very near Titan and downstream of the nearly corotating magnetospheric plasma, Ness et al. (1982) have shown that the observed magnetic field is primarily induced, resulting from the piling up and subsequent draping of Saturn's magnetospheric field.

As a result of the foregoing discussion it is possible to exclude a terrestial-like, or planetary magnetic field dominated type of interaction. Also, Titan has been known for some time to have an extensive atmosphere (Kuiper 1944), and therefore a lunar type of interaction can also be excluded. It is therefore only necessary to consider the three types of atmospheric interactions outlined in Figure 2 due to Michel (1971a). In the first (2a) the flowing plasma has a shallow component that sweeps into the ionosphere and modifies the vertical profile of the photoionization electron density. This figure would be modified for Titan to include the significantly larger collisionally induced ionization component that results when interacting with the milllion degree electrons in Saturn's magnetosphere. In this "soft" type of interaction there will be charge exchange absorption as well as mass loading of the impinging solar wind or magnetospheric plasma. The effects of these two processes on the strength and configuration of the

Titan bow shock will be discussed later.

In the second (2b) the ionospheric pressure is great enough to stand off the impinging plasma high in the ionosphere, and the resulting tangential disontinuity excludes any interaction with the ionosphere, causing negligible absorption and mass loading. In the third type of interaction (2c), in which a magnetized plasma is assumed, the highly conducting ionosphere excludes the magnetic field resulting in a pileup of magnetic field lines and formation of an induced tail field. Based upon the results of Ness et al. (1982), the interaction at Titan must have at least some of the characteristics similar to that displayed in Figure 2c. However, when the observed effects of mass loading, etc., are included it is clear that while in Saturn's magnetosphere, and probably in Saturn's magnetosheath and in the solar wind as well, the characteristics of all three types of ionosphere-atmoshere interactions can occur. (For a discussion of Titan's interaction with Saturn's magnetospheric plasma at the time of Voyager 1 see Neubauer et al., 1984).

Atmospheric Absorption and Mass Loading

When a plasma impinges on an atmosphere, absorption of the plasma occurs through charge exchange, and that portion that flows past is "mass loaded" through the pickup of cool, heavy ions. The degree with which the impinging plasma suffers absorption has a direct effect on the strength and sub-solar distance to the shock that is likely formed. Mass loading primarily affects the shape of the shock, greater mass pickup causing a blunter shock surface.

Computation of both the minimum ionopause distance and the 100% absorption flow line, below which no solar wind can penetrate as a result of charge exchange, requires a knowledge of the composition and structure of Titan's upper atmosphere. The atmosphere has been found to be composed primarily of molecular nitrogen plus either atomic or molecular hydrogen. Using the exospheric distribution for N_2 reported by Broadfoot et al. (1981), Hartle et al. (1982) have estimated the minimum ionopause distance to be about 4400 km, at which level the N_2 density is 4.5×10^5 /cm^3. For this they assumed the ionopause to be the altitude where the ion-neutral mean free path, $1/\sigma n$, equals the scale length for horizontal flow ($\cong$ 1 Titan radius, or R_T), and a value for the ion-neutral cross section, σ, of 5×10^{-15} cm^2. The

neutral density, n, is assumed to be primarily N_2 below 5000 km (see Figure 3a).

In order to estimate the maximum depth of penetration of the impinging plasma, we have computed the radius of that flow line at which the plasma is totally absorbed. Following the method outlined by Gombosi et al. (1980, 1981) applied previously to Venus, and by Russel et al. (1983) applied to Mars and Venus, we have

$$\varepsilon(h) = \sum_i n_i(h)\ \sigma_i$$

where $\varepsilon(h)$ is the probability per unit length along a flow line of a charge exchange interaction at an altitude h, $n_i(h)$ is the density of the i-th neutral species, and σ_i is the charge transfer cross section between a proton and the i-th neutral species. The number per unit area of fast solar wind ions participating in a charge exchange process while moving a distance Δs, is

$$\Delta N = - \varepsilon(h(s)) \cdot N \cdot \Delta s$$

The total fractional absorption along a flow line is then

$$L = 1 - e^{- \int_{path} \varepsilon(h(s))\ ds}$$

L is plotted in Figures 4 and 6. The total dayside absorption above a given flow line, normalized to the amount of unperturbed solar wind flow that the planet of obstacle radius R_n would absorb, can be written as:

$$\mathcal{L}_{n(h_o)} = \frac{\int_{r(h_o)}^{\infty} 2\pi\ r(h)\ L(h)\ dr}{\pi R_n^2}$$

$\mathcal{L}_{n(h_o)}$ is plotted in Figures 5 and 7. In these calculations the simple circular geometric configuration similar to that of Gombosi et al. (1980) has been used. The more accurate results obtained using flow lines derived from the work of Spreiter et al. (1978) is currently in progress, but these results are not expected to change significantly, as is apparent when the Gombosi et

al. (1980) and (1981) results are compared. Figures 4 (percent absorption along a flow line versus flow line radius) and 5 (total percent absorpion versus R_{min}) display the results obtained using the 165° K molecular nitrogen and atomic hydrogen atmospheric model of Strobel and Shemansky (1982) with solar wind conditions, and Figures 6 and 7 display the results for the same atmospheric model assuming magnetospheric plasma compositions and nearly corotational velocities, etc., consistent with Voyager observations. The 100% absorption flow lines are seen to occur at a radial distance of 4240 km under solar wind conditions and 4100 under magnetospheric plasma conditions. The corresponding absorption percentages are, respectively 20% and 25%. The velocity dependent charge exchange cross sections have been obtained from Rose and Clark (1961). For purposes of comparison, we also show as inserts in these figures the corresponding results from the two papers of Gombosi et al. (1980, 1981). The effects of magnetic fluctuations [See Gombosi et al., (1980)] have not been included. If the ionosphere has an electron-ion density of sufficient temperature to stand off the solar wind at a greater radius, the net plasma absorption will decrease accordingly.

Recently, Bertaux and Kockarts (1983) have proposed a model exosphere consisting of both molecular nitrogen and molecular hydrogen in which the density of molecular hydrogen is much greater than that in the Strobel and Shemansky model, i.e., more than a factor of 10^4 at the 4000 km level (see Figures 3b). However, although there is significantly more molecular hydrogen in the region above the 100% absorption flow line, when account is taken of the fact that atomic hydrogen undergoes a resonant charge exchange with protons whereas molecular hydrogen does not, and the effects of the velocity dependence of the cross-sections are included, the increase in absorption of the (N_2,H_2) model is not as great as one might expect. Using their model atmosphere (including a two step temperature profile of 165°K and 186°K), the 100% absorption radii and net absorpion under solar wind and magnetospheric conditions have been computed as before, resulting in the values (4140 km, 37%) and (4000 km, 19%) respectively. Hence, under all conditions we find that solar wind and magnetospheric plasma absorption at Titan are greater than at Venus.

In order to determine the conditions under which the ionosphere pressure standoff radius is greater than the 100% absorption flow line radius as well as the corresponding mass loading, we have used the method of Hartle et al.

(1982) and computed the density of ions and electrons produced by photoionization and by collisions between atmospheric neutrals and the impinging plasma. This has been done under varying conditions of pressure in terms of both the density and velocity appropriate for the solar wind (including the shocked solar wind or magnetosheath plasma) and the magnetospheric plasma. A determination of the degree of mass loading is necessary in order to determine the type (if any) of shock that will likely result. Using the velocity dependent ionization cross-sections (protons or electrons) for molecular nitrogen and for either atomic or molecular hydrogen (Rose and Clark, 1961); Banks and Kockarts, 1973) we have determined the ionopause radius assuming either 186°K or 8600°K electrons and ions, the corresponding Saturn magnetopause distance, and the degree of mass loading. The maximum values of $S/\rho v$ below which there should be no shock have been computed from Michel, (1971b), i.e.,

$$S = [\, N_e\, V_e\, \sigma_e + N_i\, V_i\, \sigma_i + J \,]\, N_o H\, m_o$$

and

$$S = k\, \rho_1\, V_1$$

where N_e, V_e, σ_e, and N_i, V_i, σ_i are the number density velocity and collisional ionization cross sections for electrons and ions, respectively, J respresents the photoionizing flux from the sun, N_o, H, m_o are the number density, scale height and mass of the atmospheric atom or molecule in question at the exobase, k is a proportionality constant, and ρ_1, V_1 are the mass density and velocity of the plasma. If k_{max}, defined by (Cloutier et al., 1978)

$$k_{max} = \frac{S_{max}}{\rho_1 V_1} = \frac{(1 - M^2)^2}{(\gamma + 1)\, M^2 [2 + (\gamma - 1) M^2]}$$

is exceeded a shock must form. Here M is the Mach number of the flow, and γ is the ratio of specific heats. For $\gamma = 5/3$ and $M \to \infty$, then $k_{max} = 0.56$ and for $M = 2$, $k_{max} = 0.18$.

The ionopause standoff distance and $S/\rho v$ ratio have been computed for different solar wind densities and speeds with the constraint that the bow

shock be located within Titan's orbital radius, or $R_{bow\ shock} < 20.2\ R_S$, and for magnetospheric plasma conditions. The results for the former are displayed in Figures 8a and b for (N_2,H) and (N_2,H_2) atmospheres, respectively. Also shown are the regions where $S/\rho v > .56$, the high Mach number minumum value of the mass loading ratio for which a shock will form. For low Mach number (a major portion of the time in the magnetosphere), the corresponding value of $S/\rho v$ is 0.18 ($M = 2$). Recalling the 100% absorption flow line results, we see that only over a very limited range of solar wind density and velocity will there be an ionopause above the critical absorption radius, and that the (N_2,H) and (N_2,H_2) models differ as to whether a shock will form, shock formation more likely occurring only for the latter model.

In like manner we have computed the same quantities corresponding to Titan interacting with magnetospheric plasma and thereby being influenced by the 200 ev electron gas and (almost) rigid corotating protons (heavy ions neglected). Both the (N_2,H) and (N_2,H_2) models predict, at most, a very weak shock. Figures 9a and b display the variation in ionopause distance with proton density corresponding to different plasma velocities for the (N_2,H) and (N_2,H_2) models. For comparison with the Voyager 1 measurements near Titan, Figures 10a and b display the electron density-plasma proton density-ionopause radius results for 186 and 8600°K electron-ion temperatures.

In the foregoing analysis, the considerable variability in the characteristics of the magnetospheric plasma (Goertz, 1983) has been neglected. The magnetoplasma conditions while Titan is in the tail region should differ considerably from those anywhere else since outflow down the tail of Saturn's magnetospheric plasma should occur here, and the field direction may undergo relatively rapid directional changes there as the tail current sheet flaps up and down in response to solar wind pressure and direction changes.

Titan Observations

There have been three opportunities to observe Titan plasma interactions, but of these, only Voyager 1 and Pioneer 11 were either near Titan or at least passed near its orbit. In both of these cases Titan was in Saturn's magnetosphere. On the other hand, occurring while Titan was in Saturn's magnetosheath, Voyager 2's flyby was at a much greater distance and occurred

well out of Titan's orbital plane. Only Voyager 1 passed close enough to Titan to conduct direct measurements of the interaction. The next best opportunity was afforded Pioneer 11, which passed roughly 20 R_T (Titan radius = 2575 km) above Titan's orbit some 145 R_T downstream.

Figure 11, from Ness et al. (1982), displays two views of the Voyager 1 trajectory near Titan along with magnetically important event intervals and a corresponding field magnitude plot. Figure 12 [from Hartle et al., (1982)] displays the sun, Saturn, and corotation directions, a Titan orbital plane projection of the plasma steamlines, and important plasma and field event intervals (compare Figures 11 and 12). Figure 12 suggests either that the flow around Titan is dissimilar on either side of the plasma flow axis, or else the flow direction changed during the short time that Voyager 1 passed through Titan's wake.

In their studies of the solar wind interaction with planets having atmospheres, Spreiter et al. (1980) describe the bow shock and magnetopause contours in terms of the parameter H/r_o, where H is the ionization scale height and r_o is the ionopause distance. Figure 13 displays scaled magnetopause and bow wave curves based upon their results that have been scaled for Titan. Their studies, however, assume a tangential discontinuity (see Figure 2b) which may not exist because of the considerable absorption noted above. It should be possible to obtain an estimate of the value of the H/r_o parameter from data related to the size of the obstacle presented by Titan to the flow. The relevant data are the energetic particle observations as well as those of the magnetic field by Ness et al. (1982). Figures 15a (from Vogt et al., 1981) and 15b (from MacLennan et al., 1982) display two energetic particle profiles. The obstacle radius due to Titan is seen to average about 3830 km, which is roughly 5-10% less than the computed 100% absorption radius, is consistent with a small value of H/R_o (see Figure 13), and suggests that the ionopause radius is not greater than the 100% absorption radius.

Kivelson and Russell (1983) have extrapolated the field vector directions obtained in the tail lobes by Voyager 1 back to a plane oriented perpendicular to the flow direction, and found that the plasma flow needed to be aberrated an average of 27^o toward Saturn at the time. Figure 14, which is a modification of their Figure 7, shows the exobase circle (3800 km radius), a 4240 km 100% absorption radius circle due to charge exchange, and an H/r_o=0.02

flow-normal plane circle radius assuming the method of Spreiter et al (1980) can be applied. Although the extrapolated lobe field lines (X's contained in the contours) in the figure should lie outside the ionopause circle, one finds that most of them can be found between this boundary and that of the exobase. This suggests that the flow and field lines are not excluded from Titan's ionosphere, and that the interaction likely is quite "soft." Certainly, (refering to Figures 2b and c) there appears to be no evidence for either a tangential discontinuity or strong exclusion of the magnetic field embedded in the impinging plasma by the ionospheric conductity. The plasma atmsophere interaction at Titan in existence during the Voyager 1 flybe would appear to be one combining the characteristics displayed in Figures 2a and c, although if the plasma flow direction was changing at the time all three types of interactions could occur.

The implied small value of H/r_o (assuming the existence of the required tangential discontinuity) suggests that H must be small and therefore, with low mass density due to ionized hydrogen above the exobase, a low temperature ionosphere at the interaction region is required. If the electrons are in equilibrium with the cool neutrals, use of the computed collisional and photoionization induced electron-ion density suggests that there will be no ionopause. A higher temperature electron component, that is not in equilibrium with the neutrals, is required in order for the ionopause to be located outside the 100% absorption radius. However, this is not consistent with the data unless variations in the flow direction of the plasma are assumed to have led to incorrect estimates of the obstacle size, i.e., H/ro.

Analysis of the EUV emission by Strobel and Shemansky (1982) requires the existence of hot (2×10^5 ^oK) secondary electrons in the atmosphere at and below the exobase, i.e., characteristic of auroral electrons. In addition, some of the emission features appear to come from narrow altitude regions (i.e., 250 km at 5000 km) and from both high and low temperature regions. They conclude that the energy deposition requirements needed to explain the EUV emission exceeds the EUV deposition rate by about a factor of 10, i.e., photoelectrons alone cannot provide the required amount of energy. The EUV results would tend to strongly favor the porous interaction model instead of a tangential discontinuity type of boundary. They also estimate that if collisional ionization occurs over the altitude range 3600-4000 km, the estimated production of N_2^+ and N^+ of 9×10^8 and 1.8×10^8 /cm^2 yields an

average electron density of about 3 X $10^3/cm^3$ for an assumed recombination coefficient of 3 X 10^{-6} cm^3/sec. This value for the electron density is consistent with the upper limit suggested by the radio occultation data of Lindal et al. (1983).

It is instructive to compare the preceding electron density with that obtained using the formula suggested by Hartle et al. (1982), where the production rate, P, is given by

$$P = (N_e V_e \sigma_1 + J) n$$

where N_e, V_e are the number density and speed, respectively, of the magnetospheric or solar wind electrons, σ = 1-2 X 10^{-16} cm^2 is the collisional ionization cross-section, J is the photoionization flux nominally about 5 X 10^{-9} sec^{-1}, and n is the neutral atom or molecule participating in the charge exchange reaction. In this calculation we are neglecting secondary electron effects. For a magnetospheric configuration, and neglecting the much slower protons or ions (the several million degree electrons have V_e about 9000 km/sec), use of this formula results in an average electron density over the 3800-4000 km height interval of about 1.8 X 10^3 cm^{-3}. Substitution of typical magnetosphere plasma values suggests that roughly 80% of the ionization is a result of collisions, i.e., collisional ionization dominates over photoionization, essentially reverse the situation at Venus. Comparison of this with the electron density estimate of Strobel and Shemansky (1982) suggests that about 40% of the electrons may have been deposited near the exobase directly from the magnetospheric plasma electron component rather than resulting from any ionization process. Strobel and Shemansky (1982) have interpreted some of the features of the EUV emission in terms of very hot electrons that exist intermitantly in the exosphere, and it is perhaps curious, then that estimates of Titan's energetic particle obstacle radius suggest a value of H/r_o that is consistent with very low temperatures. Perhaps electrons produced by collisional impact ionization with cold (160°K) molecules of nitrogen are able to cool very rapidly. Referring again to Figures 10a and b, it is seen that the smaller inferred obstacle size is consistent with a low temperature, several X $10^3/cm^3$ density, ionosphere. A high temperature, $10^3/cm^3$ ionosphere should have resulted in a larger obstacle for Titan. If the direction of flow of the magnetoplasma changed during the

Voyager 1 flyby of Titan such as to cause the effective obstacle size to be underestimated, and the ionopause radius was actually greater than the 100% absorption flow line radius, then a higher temperature ionosphere is implied. We will return to this point when discussing measurements of Titan's magnetic tail.

Assuming the higher temperature ionosphere, and therefore an ionopause that lies outside the 100% absorption radius, we have followed the method outlined in Wolff et al. (1979) and found the variability in the Titan ionopause altitude due to changes in solar EUV flux to be only of the order of 1 - 2%. Variations in the magnetospheric plasma will be the dominant factor controlling the altitude of Titan's ionopause because photoionization is only about 25% that due to collisions. The relative importance of both changes in the solar wind plasma and the solar photoionization flux at Titan should be only about 1% what they are Venus, although significant enhancements in the former can occur when stream-stream interactions persists all the way to 10 AU (Burlaga et al., 1983).

Speculations on Titan's Bow Shock

It has been suggested above that both the solar wind and magnetospheric plasma undergo significantly more charge exchange absorption in the atmosphere of Titan than in that of Venus. As a result, the shock should be weaker and the nose of the shock closer to Titan than at Venus. There may have been occasions at Venus when a weak subsolar shock surface may have moved inside the planet and with a greater absorption predicted for Titan, one would expect such a phenomenon to occur more frequently there. Another modification of the shock shape occurs when mass loading of the field lines by cold ions occurs, which results in a displacement of the shock surface away from the object in the flow-normal plane. Figure 8 suggests that under the usual high Mach number solar wind conditions, for which $S/\rho v$ must be > 0.56 in order for a shock to form, even if the solar wind pressure is great enough to push Saturn's bow shock inside Titan's orbit, the Titan shock may still be very weak or even non-existent at times of relatively high density [i.e., $>0.3/cm^3$ for the (N_2,H) model]. Under the typically low Mach number conditions occurring in the magnetosphere, the minimum value of $S/\rho v$ for a shock to form is only 0.18 ($M = 2$), and reference to Figure 9 suggests that under high

density conditions (i.e., .6 - 1./cm^3) the shock may not form even if the value of M would normally suggest that it should. That is, a shock may form at the lower values of M > 1 only if the density is low enough. For purposes of comparison, Figure 16 displays both the Titan and Saturn bow shock (neglecting mass loading in the case of the former, including the magnetopause in the case of the latter) that are consistent with a particularly energetic solar wind event [Burlaga et al. (1983)].

Possible Comet-Like Titan-Solar Wind Interaction

Some of the characteristics of comets that produce a significantly different type of interaction with the solar wind than a typical planet include the considerably larger scale height and therefore slower rate of absorption of the solar wind, and outflow velocities that are high enough to produce an internal shock (partly because the sound speed decreases with distance in response to decreasing temperature). Hence, both an external and internal shock surface can develop, either or both being fairly weak. As noted previously, high velocity plasma absorption in Titan's atmosphere is likely significantly greater than that predicted for Venus, and the weak gravity-light molecule exosphere configuration will allow for a greater gas outflow at Titan as well. Bertaux and Kockarts (1983) have computed the outflow rate for their (N_2,H_2) model and suggest a value of 5.22 X 10^{27} molecules/sec at 4100 km. This corresponds to a velocity of about 80 m/sec at 4100 km. In general,

$$v(r) = \frac{K}{4\pi r^2 n_o} e^{\frac{m g r_o}{k T}\left(1 - \frac{r_o}{r}\right)}$$

where K is the outflow rate. For molecular hydrogen at 186°K, using a value for r_o of 4100 km, we find $v(r_o) \simeq 80$ m/sec. The corresponding sound speed is about 1.13 km/sec. Since the outflow velocity should basically decrease as $1/r^2$, the only way supersonic conditions could occur is for the upper atmospheric temperature above 4100 km to rapidly decrease with altitude to an unrealistically low value of 1 or 2°K. In some comet models, it has been proposed that the temperature decreases some two orders of magnitude over 100 km (Mendis and Houpis, 1982). A similar type of temperature decrease with

altitude in the upper atmosphere of Titan is required for an internal shock to occur.

We have considered other parameters (the inner and outer radii of the contact zone, the ionization radius, etc.,) useful in discussing the solar wind-Titan interaction in cometary terms and also find that these parameters differ considerably from those of typical comets. We conclude that only in terms of solar wind absorption and mass loading will some degree of similarity be observed. We are in the process of computing more accurate values of these quantities using more realistic (i.e., flow) configurations.

Titan's Magnetic Tail and Wake

Titan's intrinsic magnetic moment has been found to be so small that only an induced bi-lobe tail configuration has been observed (Ness et al., 1982). While beyond Saturn's bow shock, Titan will usually be exposed to a solar wind in which is frozen a spiral magnetic field that is usually confined to the orbital plane of Saturn. On the average, the tight spiral angle of the interplanetary magnetic field plus sufficient conductivity in the ionosphere will result in the type of configuration displayed in Figure 17a that is due to Alfven (1957) (from Verigin et al., 1983) The neutral sheet separating the Titan toward and away tail field lobes is then oriented essentially normal to Saturn's orbital plane. When Titan is within Saturn's magnetosphere, the "external" field will usually be oriented perpendicular to Titan's orbital plane, and the neutral plane of the induced bi-lobe tail will lie in Titan's orbital plane, or somewhat perpendicular to the solar-wind configuration [Figures 17b and c, from Verigin et al., (1983)]. However, because of the weakened dipolar field at 20.2 R_S and relatively strong azimuthal and tail-like or radial sheet currents that are frequently observed in Saturn's magnetosphere (Wilson et al., 1983), considerable angular rotation of Titan's induced tail neutral plane about the corotational direction should occur at times when these currents move past Titan.

Some predictions can be made assuming that some of geometric features, etc., of the interaction at Venus can be scaled to Titan. For example, referring to Gombosi et al. (1980) (their Fig. 1), one might expect a magnetic field versus distance along the subsolar line for Titan that is similar to that displayed in Figure 18. That is, a nominal 0.3 nT interplanetary field,

oriented predominately in the azimuthal direction because of tightening of the spiral, models to a field of about 2 nT at the bow shock, and 3 nT at the ionopause. In order to estimate the scaling factor relating the nominal lobe strength in the induced tail field to that in the magnetopause we refer to the measurements of Acuna and Ness (1982).

Ness et al. (1982) found that the inbound lobe was weaker but broader than the outbound lobe, i.e., (w = 3230 km, B = 3.25 nT) and (w = 1440 km, B = 6.7 nT), respectively. These data have been interpreted in terms of tail lobes that are much taller than they are wide (Ness et al., 1982). For example, one notes that the two w-B products agree to within 10%, and for purposes of geometric simplicity it is tempting to assume that the vertical extents of the two tail lobes are the same. Conservation of flux assuming a flux ring of radius R_o and width $\Delta R \simeq H = 0.02\ R_o$ in the flow-normal plane suggests that the vertical extent, h, of the lobes must be about 4800 km if it is assumed that little flux is "lost" as a result of field lines closing crossing the neutral sheet within 2.6 R_T behind Titan. It is interesting to note that $\sqrt{wh} \simeq R_o$.

On the other hand, it is tempting to assume that the difference in the lobe width may, in large part, have been the result of a change in direction of the flow that occurred as Voyager 1 passed through Titan's magnetic tail. That is, if one assumes a circular tail, conservation of flux, and the field profile of Figure 20, then if R_o is 4000 km and $\Delta R \simeq H$ (= 0.02 R_o) the size of the first lobe suggests a tail field of about 3.1 nT, while the second lobe suggests a lobe field of about 15.4 nT, i.e., good agreement with measurements of the field of the first lobe but poor agreement with that of the second. If one assumes that the flow direction changed during the Voyager 1 encounter of Titan in such a way that the lobe widths were underestimated (i.e., that the radially inward component of the flow decreased during the flyby), then a 50% increase in the width of the second lobe results in the predicted tail field of both agree closely with the data. Allowance for a possible flow direction change that caused <u>both</u> lobe widths to appear smaller than they actually were could result in actual lobe radii more consistent with parallel lobe field lines and a larger flow-normal ring thickness, ΔR. Differences in the two lobes could result entirely from the effects of differing <u>mass loading</u> effects caused by the interaction of the magnetized plasma with an assymetrically ionized atmosphere [Neubauer et al. (1984)]. However, while in the

magnetosphere most of the ionization of Titan's atmosphere is collisional (roughly 80%) rather than electromagnetic and hence, the difference between the day and night ionospheres may not be very large. Regardless of the details of the interaction, the average tail field observed by Voyager 1 is very nearly the same strength as the field of the magnetized plasma, and therefore, under the solar wind conditions outlined above, the tail field near Titan is likely to be roughly the same as the field frozen into the solar wind, or about 0.3 nT.

Pioneer 11 passed near Titan's orbit some 145 R_T downstream at a time when relatively strong azimuthal and radial or dayside tail-like currents were flowing in the vicinity of Saturn's equatorial plane. These current systems moved somewhat independently, but both seemed to be moving up and down perpendicular to Titan's orbit and were therefore sweeping past Titan and the spacecraft prior to, during, and after Pioneer 11 crossed Titan's orbit. Consequently, it has been difficult to separate effects that are strictly due to these current sheets from purely Titan effects, and even from possible conductance effects on these currents due to Titan's tail or some of its remanent plume material. Jones et al. (1980) have suggested that the data near the Titan orbit crossing were consistent with passage of Pioneer 11 through a possible Titan wake. This interpretation was based upon a comparison of some of the features of the Titan interval with several candidate flucutations in the field that occurred prior to and after the event in question. It was pointed out that preliminary estimates of the composition of the magnetoplasma at the time were consistent with the possible detection of a weak shock based upon changes in field directions, whereas the suggested possibiliy of passage through the wake was based on the somewhat unique character of the field variability of the interval in question. It should also be mentioned that at the time of the Pioneer 11 measurements very little photoionization was occurring in the same hemisphere as that in which most of the collisional ionization was occurring. However, the geometry was such that more photoionization and subsequent mass loading, etc. effects should have been observed before Pioneer 11 passed Titan's orbit, which is consistent with the data (Jones, 1980).

Comparison of the magnetic field observed during the Pioneer 11 Titan interval with predicted field changes due to azimuthal and tail-like currents that successfully model the remaining portion of the outbound perturbation

field $(\vec{B}_{total} - \vec{B}_{planetary})$ also suggest that the Titan interval is unique, particularly in terms of the ϕ component of the field. Figures 19a and b (from Wilson et al., 1983) compare r and ϕ components predicted by a computer derived model current system with that of the data. The manner in which the field varies during the Titan interval is seen to be particularly anomalous when compared to the preceding interval (the following interval displays effects that may be the result of approaching the magnetopause boundary layer). Since Pioneer 11 passed above Titan's orbital plane, and the "input field" is primarily due to the planetary dipole field, (i.e., a vertical field), Pioneer 11 should observe primarily a lobe field that shows up as an azimuthal, or ϕ perturbation.

Eviatar et al., (1982) have suggested that the Voyager data are consistent with the existence of plumes containing signicant amounts of heavy ion gas from Titan that have sufficiently long lifetimes to allow for them to wrap around the planet and thereby participate in the magnetospheric plasma-Titan interaction. However, an alternate interpretation of these data has been proposed by Goertz (1983). If such long-lived plumes do exist, then Titan could interact with this heavy ion materal and when account is taken of various possibilities in terms of composition, number density and temperature, it is clear that at times it is possible that the Titan-mangetospheric plasma interaction can be described in terms of Mach numbers greater than 1. Also, at times when the field is weakest (at the center of the several current sheets mentioned above) and Titan is immersed in one of its high density plumes, the flow could also be described as superalfvenic. Under such conditions, the observation of wake phenomena at large distances downstream from Titan would appear to be a distinct possibility. Such may have occurred coincident with the passage of Pioneer 11 near Titan's orbit.

Acknowledgements

We wish to acknowledge helpful discussions with J.A. Slavin, B.T. Tsurutani, and G.L. Siscoe. This research was supported, in part, by the NASA-Ames under research grant NAG 2-145.

References

Acuna, M.H., and N.F. Ness, The magnetic field of Saturn: Pioneer II observations, Science, 207, 444, 1980.

Alfven, H. On the theory of comet tails, Tellus, 9, 92, 1957.

Banks, P.M. and Kockarts, G. Aeronomy Part A, Academic Press, pp. 184-239, New York 1973.

Bertaux, J.L. and G. Kockarts, Distribution of molecular hydrogen in the atmosphere of Titan, J. Geophys. Res., 88, 8716-8720, 1983.

Broadfoot, A.L., et al., Extreme ultraviolet observations from Voyager 1 encounter with Saturn, Science, 212, 206, 1981.

Burlaga, L.F., R. Schwenn and H. Rosenbauer, Dynamical evolution of interplanetary magnetic fields and flows between 0.3 AU and 8.5 AU: Entrainment, Geophys. Res. Lett., 10, 413-416, 1983.

Cloutier, P.A., M.R. McElroy and F.C. Michel, Modification of the Martian ionosphere by the solar wind, J. Geophs. Res., 74, 6215-6228, 1969.

Cloutier, P.A., R.E. Daniell, Jr., A.J. Dessler, and T.W. Hill, A cometary model for Io, Astrophys. and Space Sci., 55, 93-112, 1978.

Eviatar, A., G.L. Siscoe, J.D. Scudder, E.C. Sittler, Jr., J.D. Sullivan, The plumes of Titan, J. Geophys. Res., 87, 8091-8103, 1982.

Geortz, C.K. Detached plasma in Saturn's front side magnetosphere, Geophys. Res. Lett. 10, 455-458, 1983.

Gombosi, T.I., T.E. Cravens, A.F. Nagy, R.C. Elphic and C.T. Russell, Solar wind absorption by Venus, J. Geophys. Res., 85, 7747-7753, 1980.

Gombosi, T.I., M. Horanyi, T.E. Cravens, A.F. Nagy, and C.T. Russell, The role

of charge exchange in the solar wind absoprtion by Venus, Geophys. Res. Lett., 8, 1265-1268, 1981.

Hartle, R.E., E.C. Sittler, Jr., K.W. Ogilvie, J.D. Scudder, A.J. Lazarus, and S.K. Atreya, Titans ion exosphere observed from Voyager, J. Geophys. Res, 87, 1383, 1982.

Jones, D.E., B.T. Tsurutani, E.J. Smith, R.J. Walker, and C.P. Sonett, A possible magnetic wake of Titan: Pioneer II Observations, J. Geophys. Res., 85, 5835-5840, 1980.

Kuiper, G.P. Titan: A satellite with an atmosphere, Astrophys. J., 100, 378, 1944.

Kivelson, M.G., and C.T. Russell, The interaction of flowing plasmas with planetary ionospheres: A Titan-Venus comparison, J. Geophys. Res., 88, 49-57, 1983.

Lindal, G.F., G.E. Wood, H.B. Hotz, D.N. Sweetnam, V.R. Eshleman, and G.L. Tyler, The atmosphere of Titan: An analysis of the Voyager 1 radio occultation measurements, Icarus, 53, 348-363, 1983.

MacLennan, C.G., L.J. Lanzerotti, S.M. Krimigis, R.P. Lepping, and N.F. Ness, Effects of Titan on trapped particles in Saturn's magnetosphere, J. Geophys. Res., 87, 4111, 1982.

Mendis, D.A., and H.L.F. Houpis, The cometary atmosphere and its interaction with the solar wind, Rev. Geophys. Space Sci., 20, 885-928, 1982.

Michel, F.C. Solar wind interaction with planetary atmospheres, Rev. Geophys. Space Phys., 16, 427-435, 1971a.

Michel, F.C. Solar-wind-induced mass loss from magnetic field-free planets, Planet Space Sci., 24, 1580-1583, 197b.

Ness, N.F., M.H. Acuna, R.P. Lepping, J.E.P. Connerney, K.W. Behannon, L.F.

Burlaga, and F.M. Neubauer, Preliminary results at Saturn from the magnetic field experiment on Voyager 1, Science, 205, 211, 1981.

Ness, N.F., M.H. Acuna, K.W. Behannon, and F.M. Neubauer, The induced magnetosphere of Titan, J. Geophys. Res., 87, 1369, 1982.

Neubauer, F.M. Possible strengths of dynamo magnetic fields of the Galilean satellites and of Titan, Geophys. Res. Lett., 5, 905, 1978.

Neubauer, F.M., D.A. Gurnett, J.D. Sudder, R.E. Hartle, Titan's magnetosphere interaction in Saturn, edited by T. Gehrels, p._____, University of Arizona press,Tucson, 1984.

Rose, D.J. and M. Clark, Jr., Plasmas and Controlled Fuscon, The M.I.T. Press, Cambridge, Mass. and John Wiley and Sons, Inc., pp. 29-53, New York, 1961.

Russell, C.T., T.I. Gombosi, M. Horyani, T.E. Cravens and A.F. Nagy, Charge-Exchange in the magnetosheaths of Venus and Mars: A comparison, Geophys. Res. Lett., 10, 163-164, 1983.

Slavin, J.A., J.R. Spreiter and E.J. Smith, A comparative study of the solar wind interaction with Jupiter and Saturn, (1984 submitted).

Spreiter, J.R. and S.S. Stahara, Solar wind flow past Venus: Theory and comparisons, J. Geophys. Res., 85, 7715, 1980.

Strobel, D.F. and D.E. Shemansky, EUV emission from Titan's upper atmosphere: Voyager 1 encounter, J. Geophys. Res., 87, 1361, 1982.

Verigin, M.I., K.I. Gringauz, and N.F. Ness, Comparison of induced magnetospheres at Venus and Titan, (1983 in preparation).

Vogt, R.E., D.L. Chenett, A.C. Cummings, T.L. Garrard, E.C. Stone, A.W. Schardt, J.H. Trainor, N. Lai, and F.B. McDonald, Energetic charged particles in Saturn's magnetosphere: Voyager 1 results, Science, 212, 231, 1981.

Wilson, G.R., D.E. Jones and B.T. Thomas, Modelling Saturn's magnetosphere and planetary magnetic field: Pioneer 11, (paper presented at the Fall AGU meeting, San Franciscio, Calif., December, 1983).

Wolf, D.F. and F.M. Neubauer, Titan's highly variable plasma environment, J. Geophys. Res., 87, 881-886, 1982.

Wolff, R.S., B.E. Goldstein, and S. Kumar, A model of the variability of the Venus ionopause altitude, Geophys. Res. Lett., 6, 353-356, 1979.

Figure Captions

Figure 1: Histogram of the frequency of occurrance of a specific value of the Saturn magnetopause distance, R_N, based upon 1275 observations of the solar wind extrapolated to the vicinity of Saturn (after Slavin et al., 1983).

Figure 2: Solar wind flow patterns in the vicinity of non-magnetic planets having atmospheres in terms of a) direct interaction; b) tangential discontinuity; and c) magnetic barrier (after Michel, 1971a).

Figure 3: a) Model atmospheric distributions of N_2 and H for Titan (after Hartle et al., 1982); b) Model atmospheric distributions of N_2 and H_2 for Titan (after Bertaux and Kockarts, 1983).

Figure 4: Absorption of solar wind plasma in the atmosphere of Titan due to charge exchange along a circular flow line as a function of flow line radius due to the (N_2,H) model used by Hartle et al. (1982). The inset figure shows the results for Venus obtained by Gombosi et al. (1981).

Figure 5: Total absorption of solar wind plasma in the atmosphere of Titan due to charge exchange absorption by the (N_2,H) model used by Hartle et al. (1982). The inset figure shows the results for Venus obtained by Gombosi et al. (1980).

Figure 6: Same as for Figure 4 except that the absorption is of magnetospheric plasma.

Figure 7: Same as for Figure 5 except that the absorption is of magnetospheric plasma.

Figure 8: a) Contours of ionopause distance versus incident proton density at constant solar wind velocity using the (N_2,H) atmosphere of Hartle et al. (1982). Also shown are the corresponding values of the mass loading ratio corresponding to a large Mach number flow. Regions where Titan is located in the free streaming solar wind (left diagonal) and where a shock must form (right diagonal) are also shown. An ionospheric temperature of 8600°K has

been assumed. Figure 8b is the same as 8a, except the (N_2,H_2) atmosphere of Bertaux and Kockarts (1983) is used.

Figure 9: Similar to Figures 8a and 8b, except magnetosphere plasma conditions and the region of shock region is not formed, although the 100% absorption radius has.

Figure 10: Ionopause electron density versus magnetospheric plasma proton density at constant flow velocity for high (8600°K) and low (186°K) ionospheres. Also shown are the corresponding ionopause radii. Voyager 1 observations near Titan would tend to favor the low temperature - high electron density model.

Figure 11: Magnitude of magnetic field observed near Titan closest approach. Upper panels display the trajectory in Titan-centered coordinates with the Y axis directed radially outward from Saturn, Z parallel to Saturn's rotation axis, and X "upstream" from the corotating magnetosphere. L_1 and L_2 refer to the northern and southern magnetic tail lobes. A may be a feature related to the dayside hydrogen corona, B and D to the inbound and outbound crossings of the tail boundaries, and C to the current sheet separating the northern and southern tail lobes.

Figure 12: Idealized plasma flow around Titan. L_1 and L_2 refer to the northern and southern magnetic tail lobes. The shaded bars refer to minima corresponding to magnetopause and neutral sheet crossings. The trajectory of a proton is approximately to scale in the observed magnetic field (after Hartle et al., 1982).

Figure 13: Scaled ionopause and bow wave contours for Titan corresponding to several values of the H/R_o parameter (based upon Spreiter et al., 1980).

FIgure 14: (Top) Projection of Voyager 1 trajectory near Titan into a plane oriented transverse to the flow (27° inward from corotational). Titan is represented by a circle, and distances are labeled in kilometers. Positions along the trajectory are assigned numbers from -55 to 39. (Bottom) Mappings of

figure along the measured magnetic field directions. Numbers given to mapped points correspond to their source location along the trajectory [from Kivelson and Russell (1983), their Figure 7]. Also shown are the exobase, ionopause radius assuming only charge exchange for an (H_2,H) atmosphere, and the corresponding ionopause circle in this flow-normal plane as inferred from Figure 13.

Figure 15: a) Counting rate versus time curves for flux of > 0.43 MeV protons measured by Voyager 1 along its trajectory as displayed in the upper curve (after Vogt et al., 1981), and b) velocity versus time contours for several ion energy ranges and the corresponding position of Voyager 1 relative to Titan (after MacLennan et al., 1982).

FIgure 16: A figure comparing the Titan and Saturn bow shocks under solar wind conditions that are sufficient to push the latter within Titan's orbit. The Titan bow shock corresponds to high Mach number conditions, and the Saturn boudaries are consistent with the bow shock and magnetopause studies of Slavin et al. (1983)

Figure 17: Sketches of magnetic lines of force and current systems associated with solar wind interaction with (a) comets (Alfven, 1957), (b) Venus (Yeroshenko, 1979) and (c) Venus (Gringauz, 1981) [after Verigin et al., 1983)].

Figure 18: Scaled magnetic field profile in the shock-ionopause, etc., region along the noon meridian for Titan as scaled from the corresponding figure for Venus by Gombosi et al., 1980.

Figure 19: a) Modelled (dashed) and measured (solid) radial and b) azimuthal perturbation field variations due to a dayside tail-like sheet current that moved up and down past Pioneer 11 as it traversed the outbound magnetosphere of Saturn near Titan. The apparently anomalous interval is contained in the several R_S region spanning 20 R_S and appears mostly in the azimuthal component.

SOLAR WIND STAND-OFF DISTANCE AT SATURN

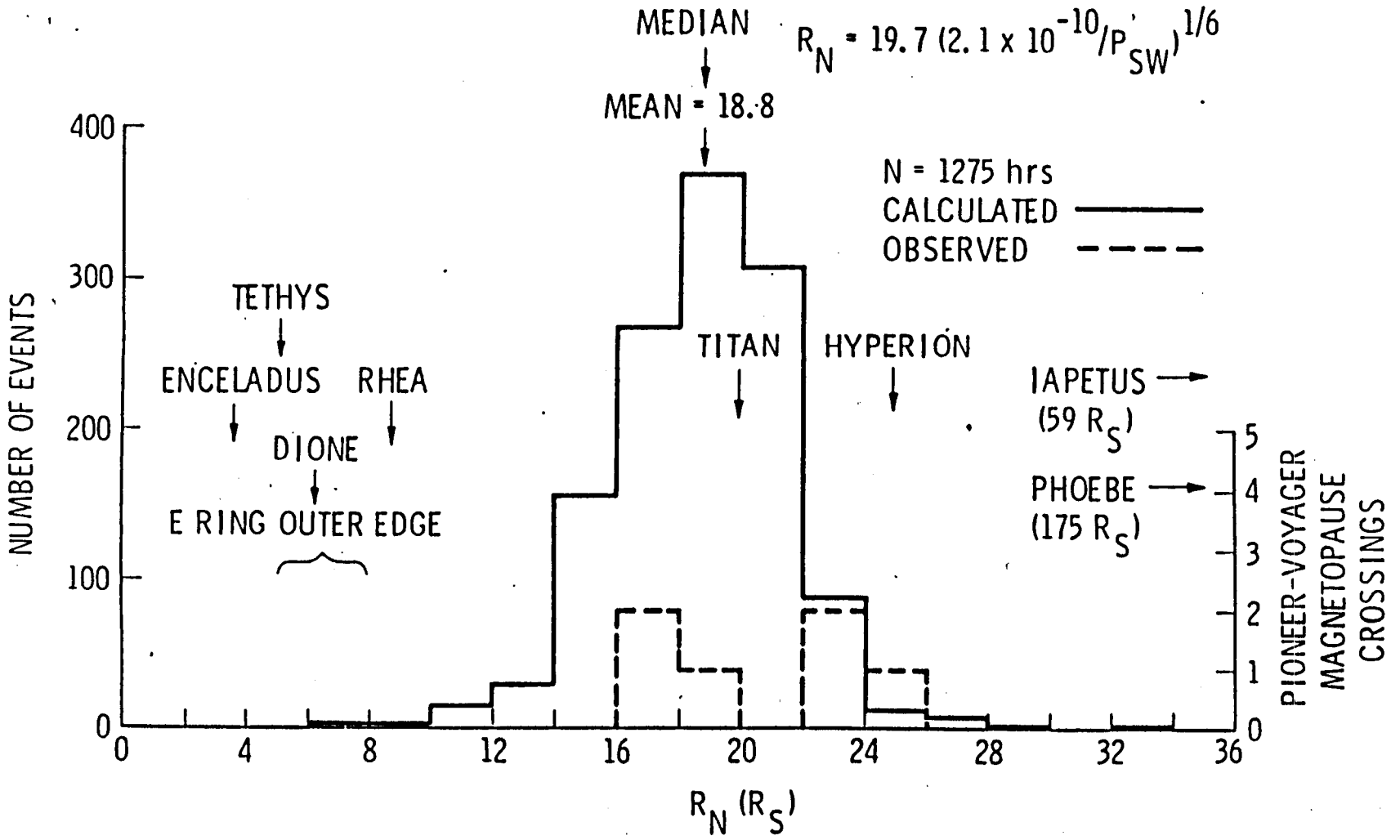

Figure 1. SLAVIN, ET AL. "A COMPARATIVE STUDY OF THE SOLAR WIND INTERACTION WITH JUPITER AND SATURN" (IN PREPARATION)

SOLAR WIND INTERACTION WITH PLANETARY ATMOSPHERES

MICHEL, REV. GEOPHYS. SPACE PHYSICS, 9, 427, 1971

(A) DIRECT INTERACTION: INFLOW RESTRICTED BY PHOTOION PRODUCTION, SOLAR WIND HAS SHALLOW COMPONENT THAT SWEEPS INTO THE IONOSPHERE.

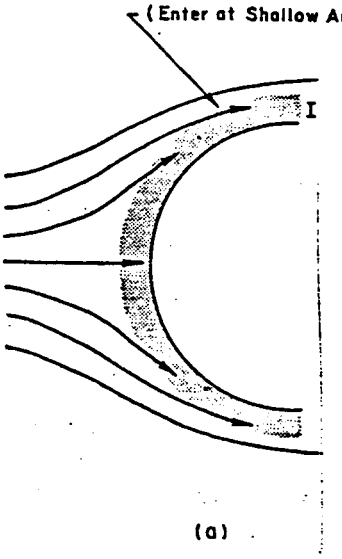

(a)

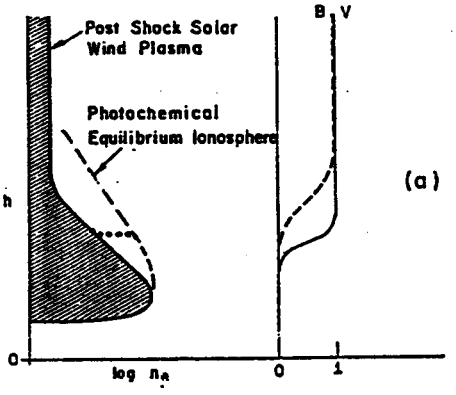

(B) TANGENTIAL DISCONTINUITY: IONOSPHERIC PLASMA EXCLUDES SOLAR WIND PLASMA, AN IMPENETRABLE INTERFACE (IONOSPHERE NKT PRESSURE EQUALS SOLAR WIND PRESSURE)

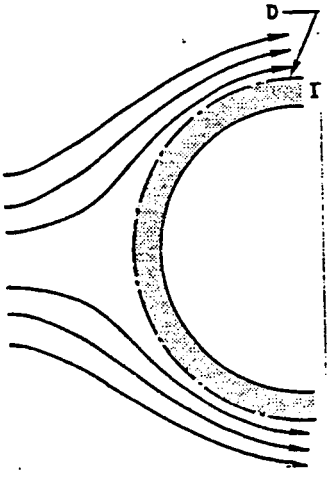

(b)

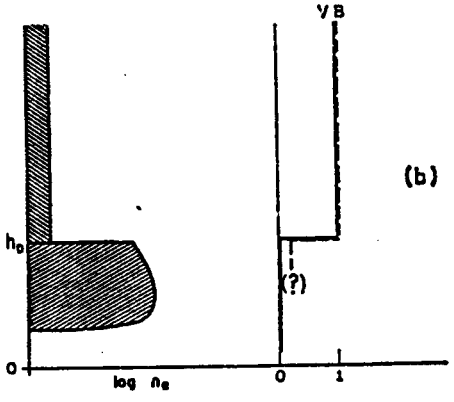

(C) MAGNETIC BARRIER: MAGNETIC FIELD LINES ACCUMULATE ABOVE HIGHLY CONDUCTING IONOSPHERE, NO DIRECT ACTION BETWEEN SOLAR WIND AND ATMOSPHERE

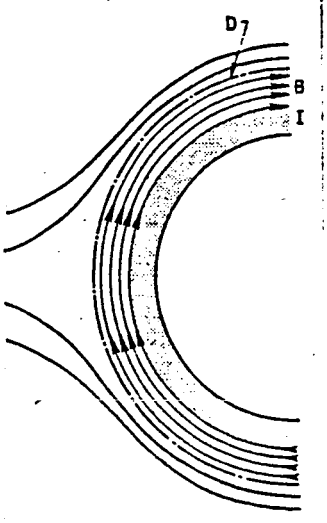

(c)

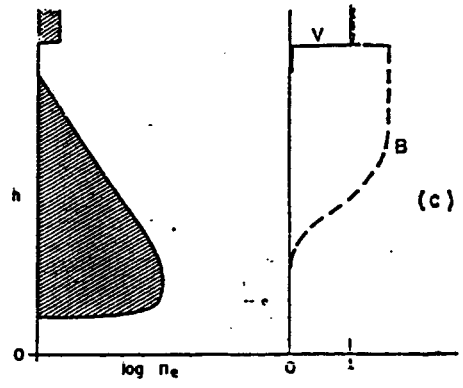

Figure 2.

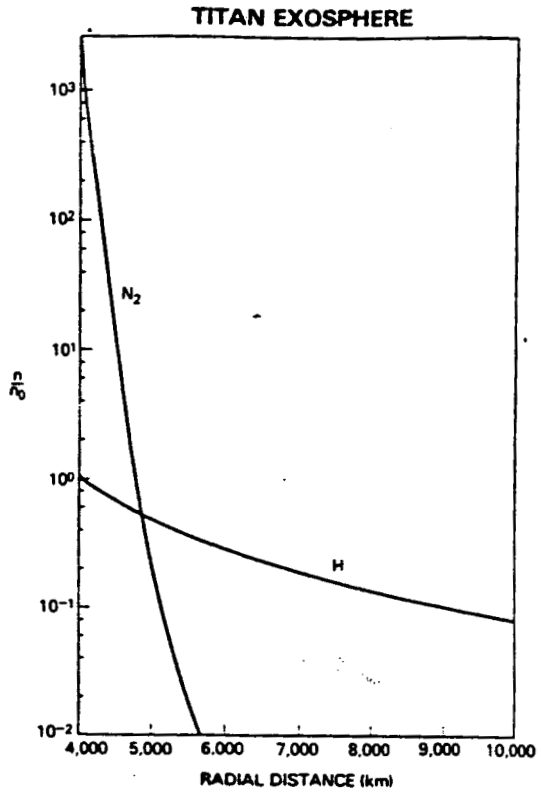

Figure 3a

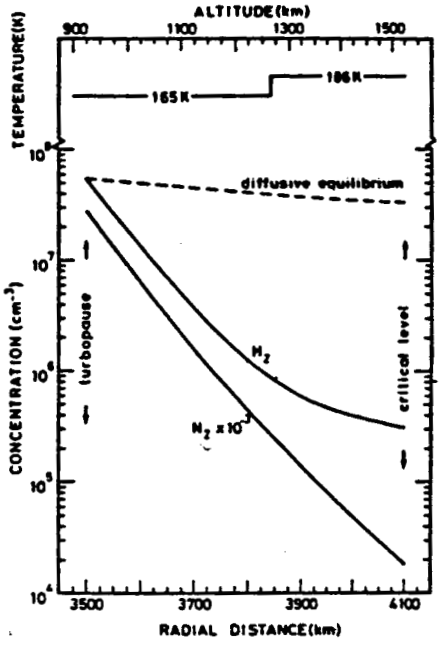

Figure 3b

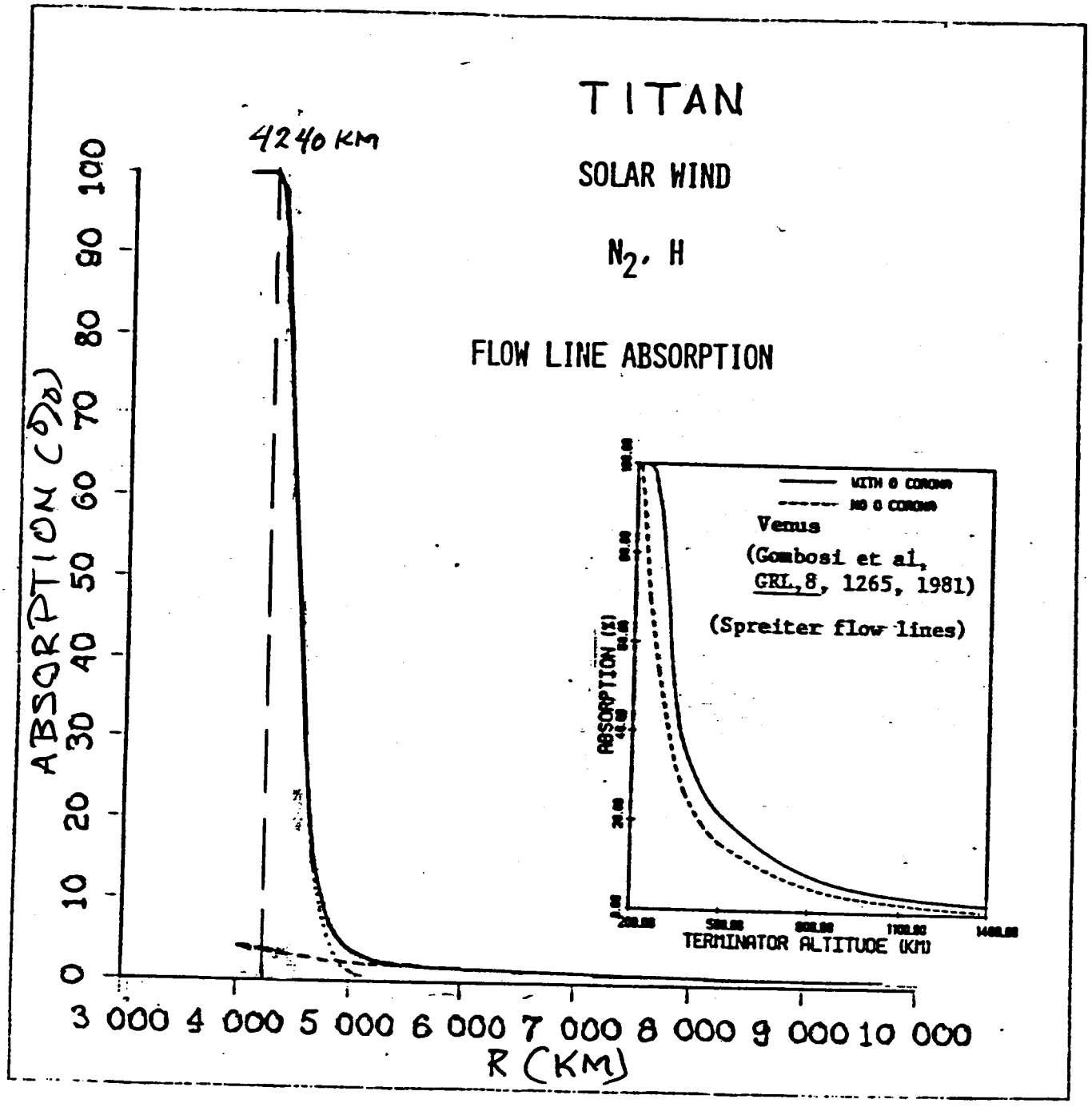
TITAN
SOLAR WIND
N_2, H
FLOW LINE ABSORPTION
4240 KM
ABSORPTION (Rd)
0 10 20 30 40 50 60 70 80 90 100
3 000 4 000 5 000 6 000 7 000 8 000 9 000 10 000
R (KM)
WITH O CORONA
NO O CORONA
Venus
(Gombosi et al, GRL, 8, 1265, 1981)
(Spreiter flow lines)
ABSORPTION (%)
TERMINATOR ALTITUDE (KM)

Figure 4

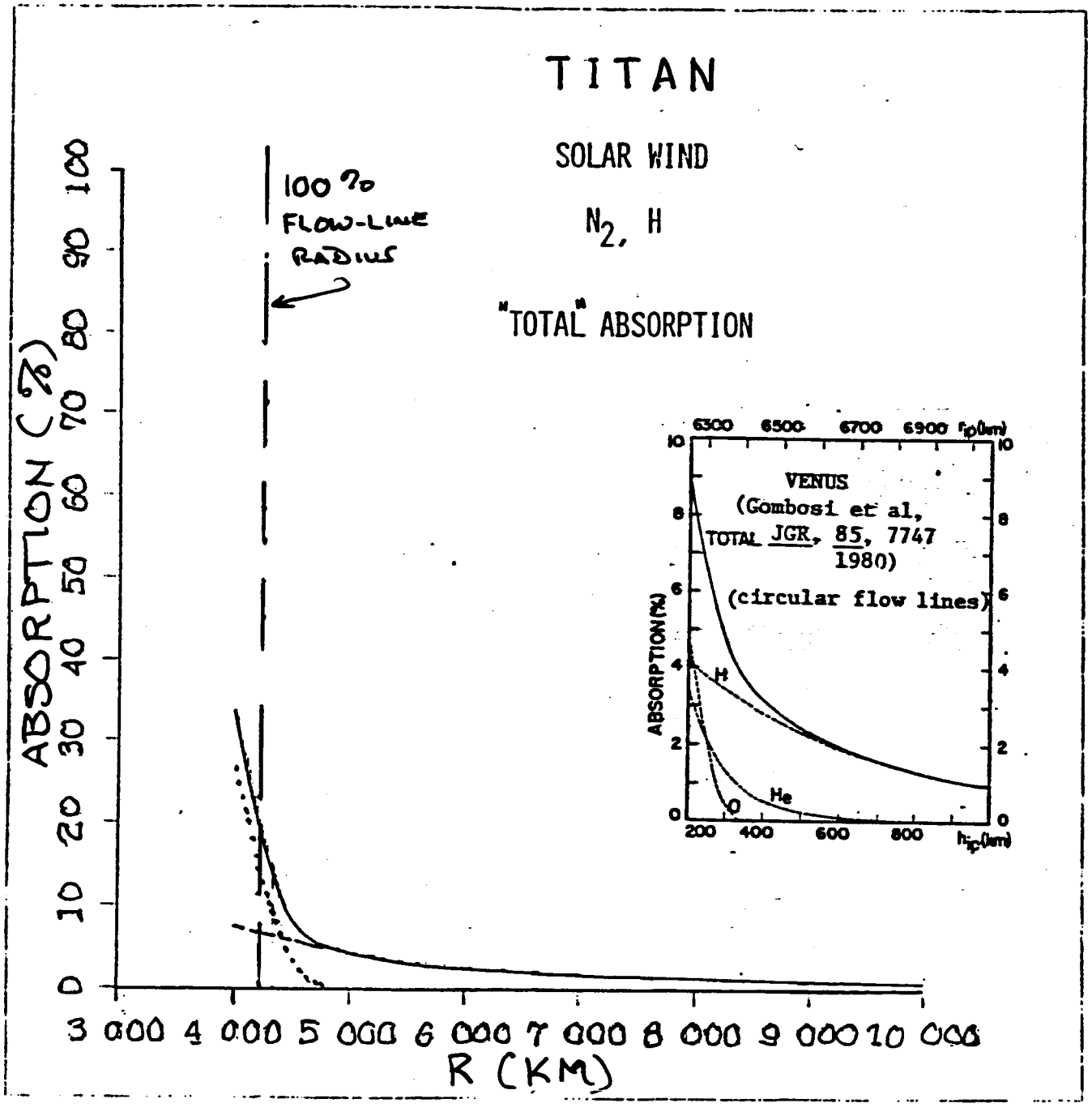
TITAN
SOLAR WIND
N_2, H
"TOTAL" ABSORPTION
100 % FLOW-LINE RADIUS
ABSORPTION (%)
0 10 20 30 40 50 60 70 80 90 100
3 000 4 000 5 000 6 000 7 000 8 000 9 000 10 000
R (KM)
VENUS
(Gombosi et al, JGR, 85, 7747 1980)
(circular flow lines)
TOTAL
H
He
O
ABSORPTION(%)
6300 6500 6700 6900 r_{ip}(km)
200 400 600 800 h_{ip}(km)

Figure 5

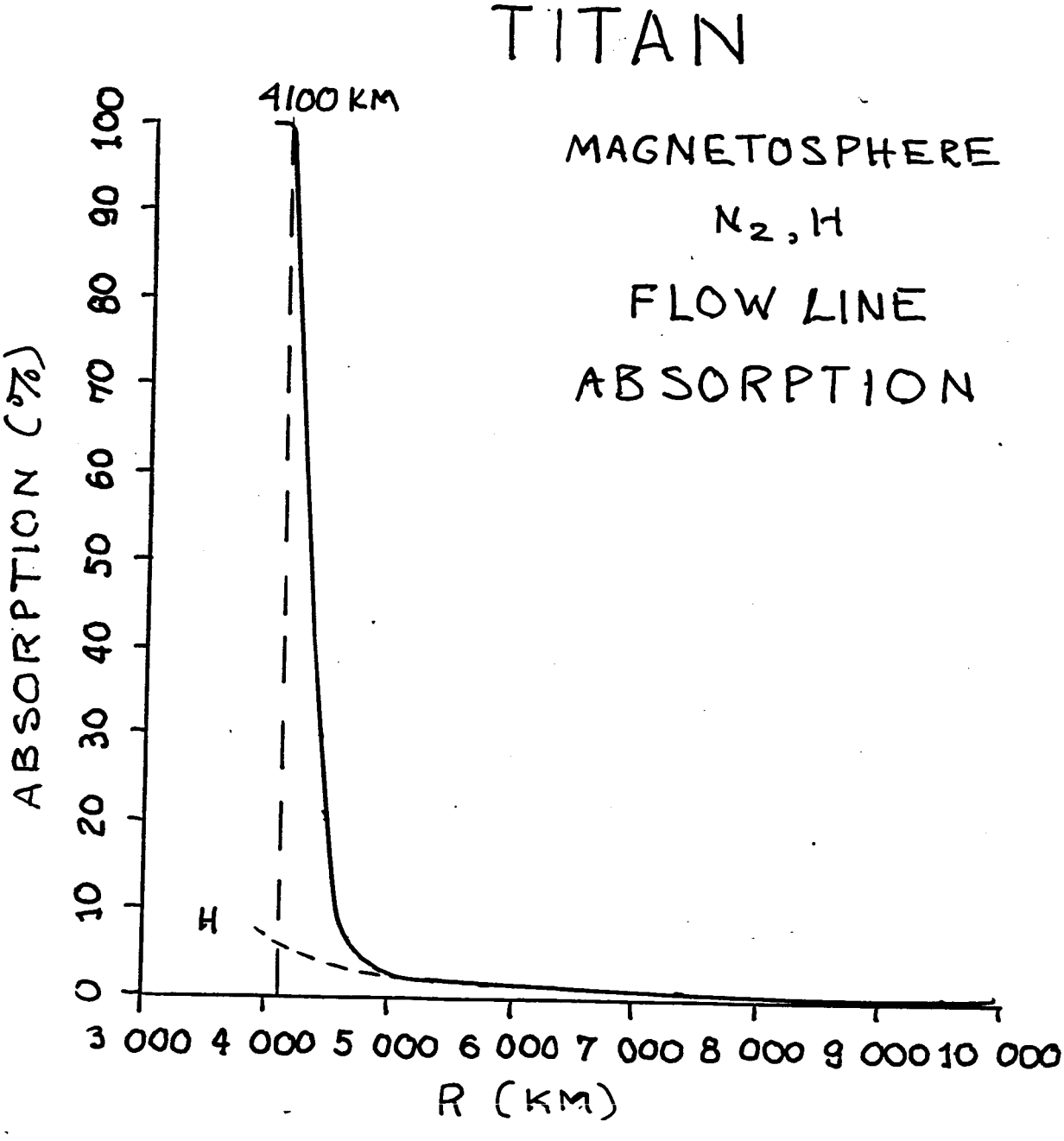
TITAN
4100 KM
MAGNETOSPHERE
N_2, H
FLOW LINE
ABSORPTION
ABSORPTION (%)
0
10
20
30
40
50
60
70
80
90
100
H
3 000
4 000
5 000
6 000
7 000
8 000
9 000
10 000
R (KM)

Figure 6

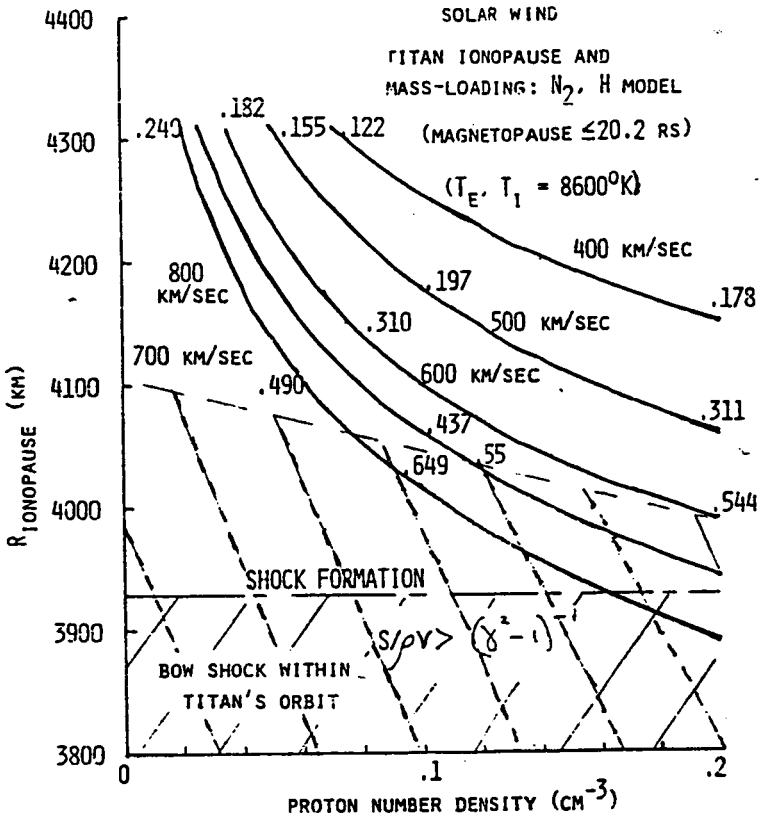

Figure 8a.

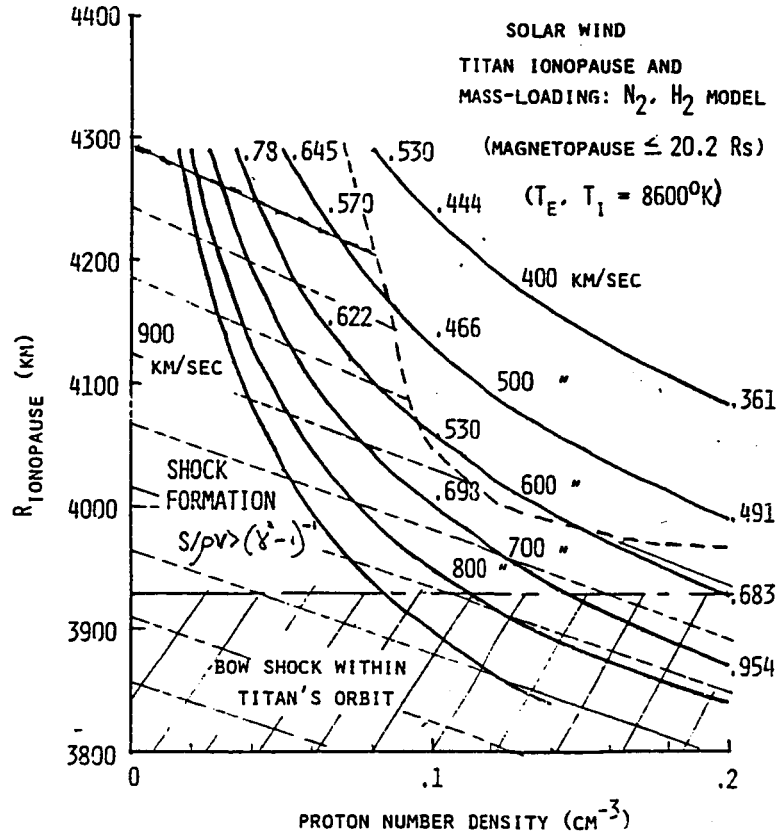

Figure 8b.

TITAN

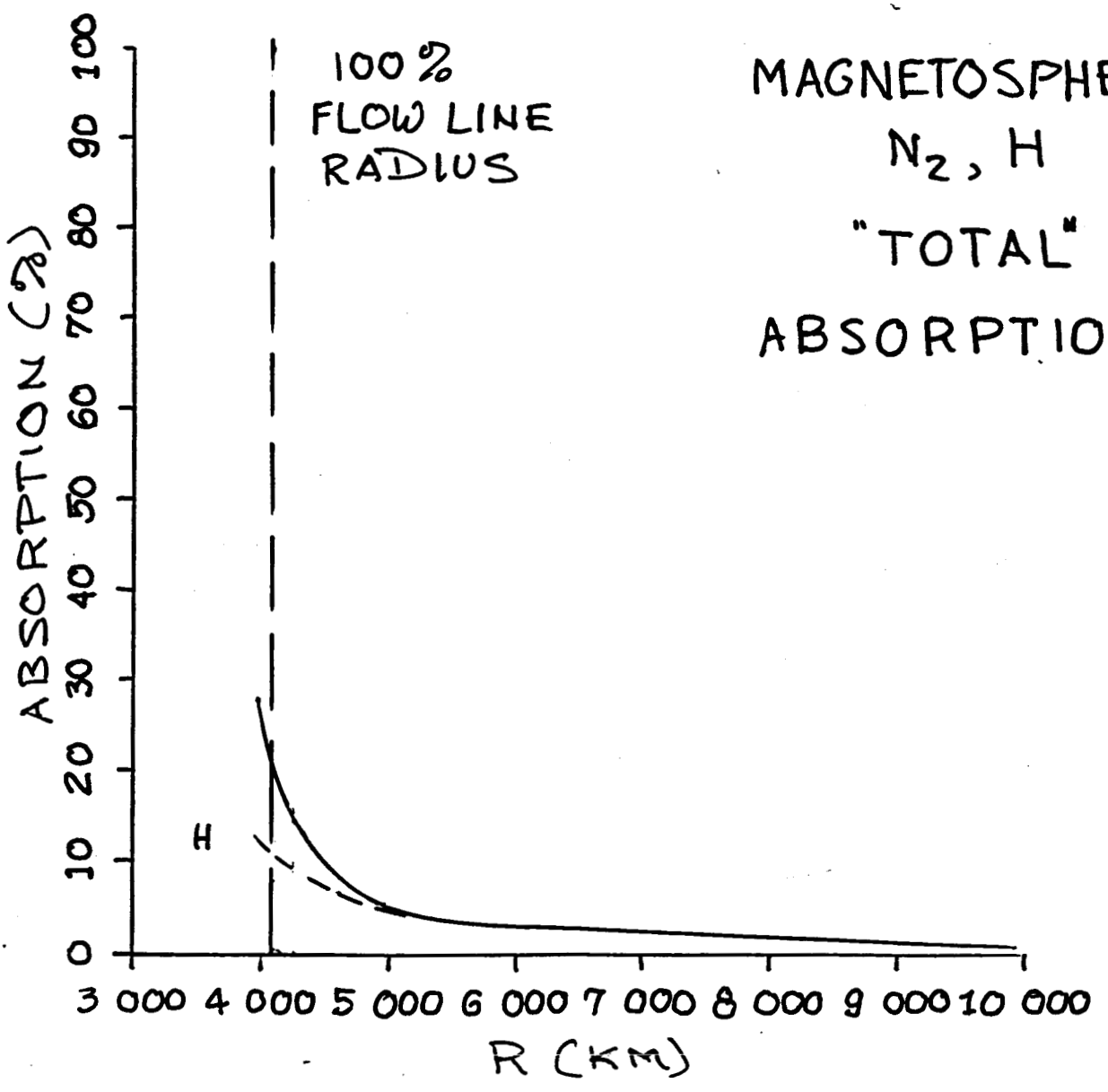

Figure 7

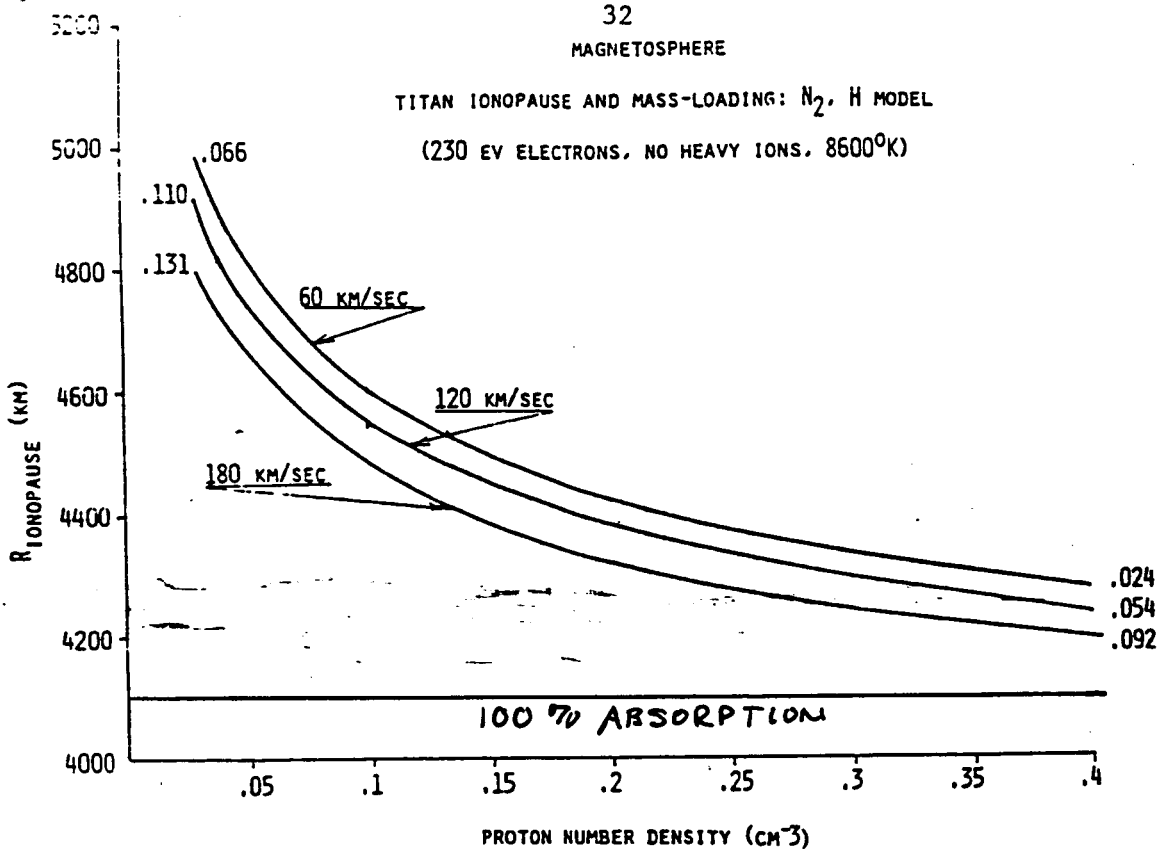

Figure 9b

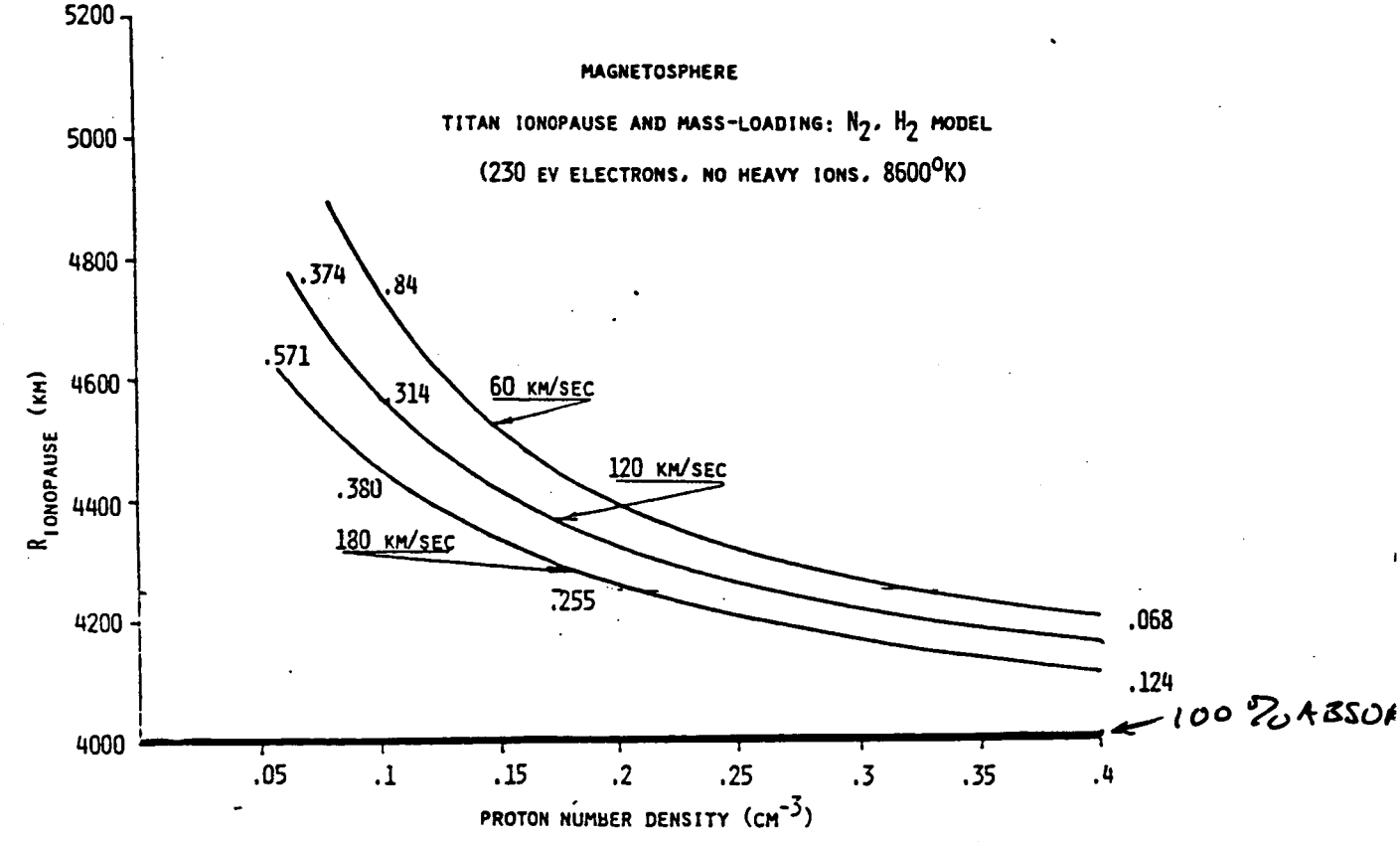

Figure 9b

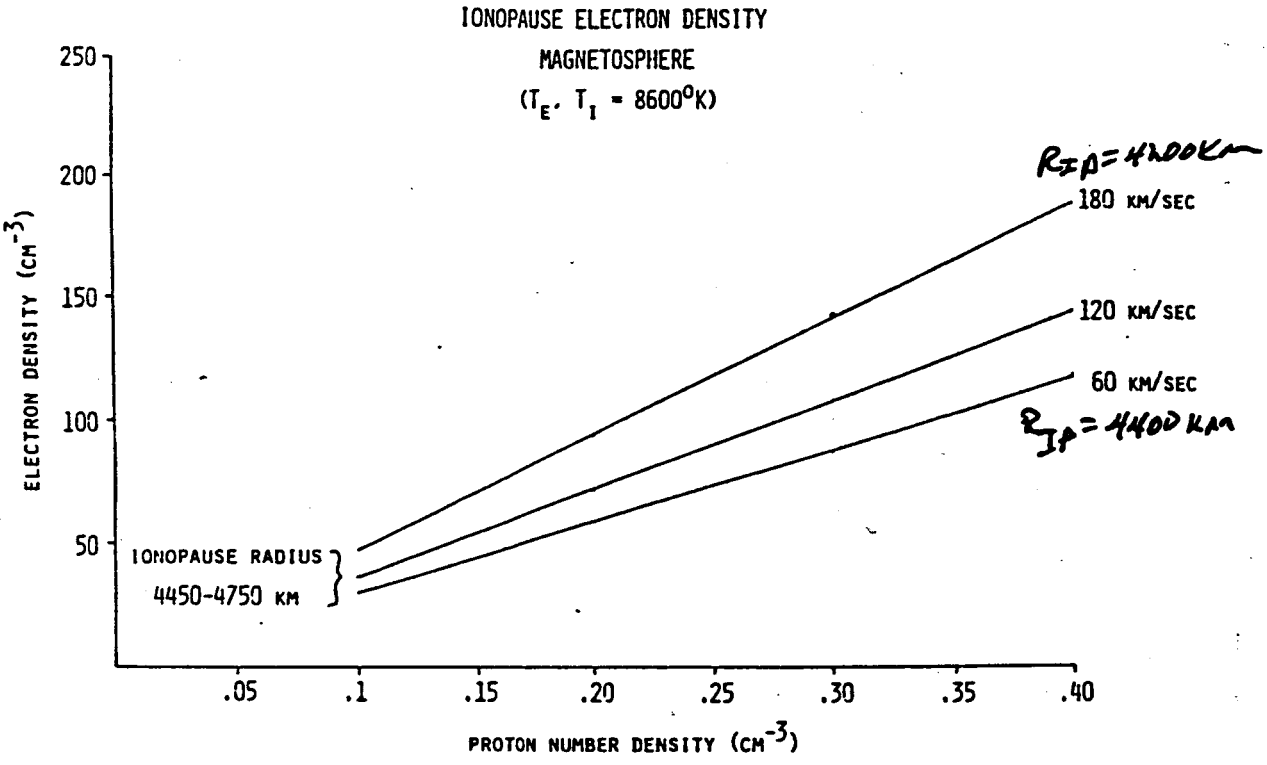

Figure 10a

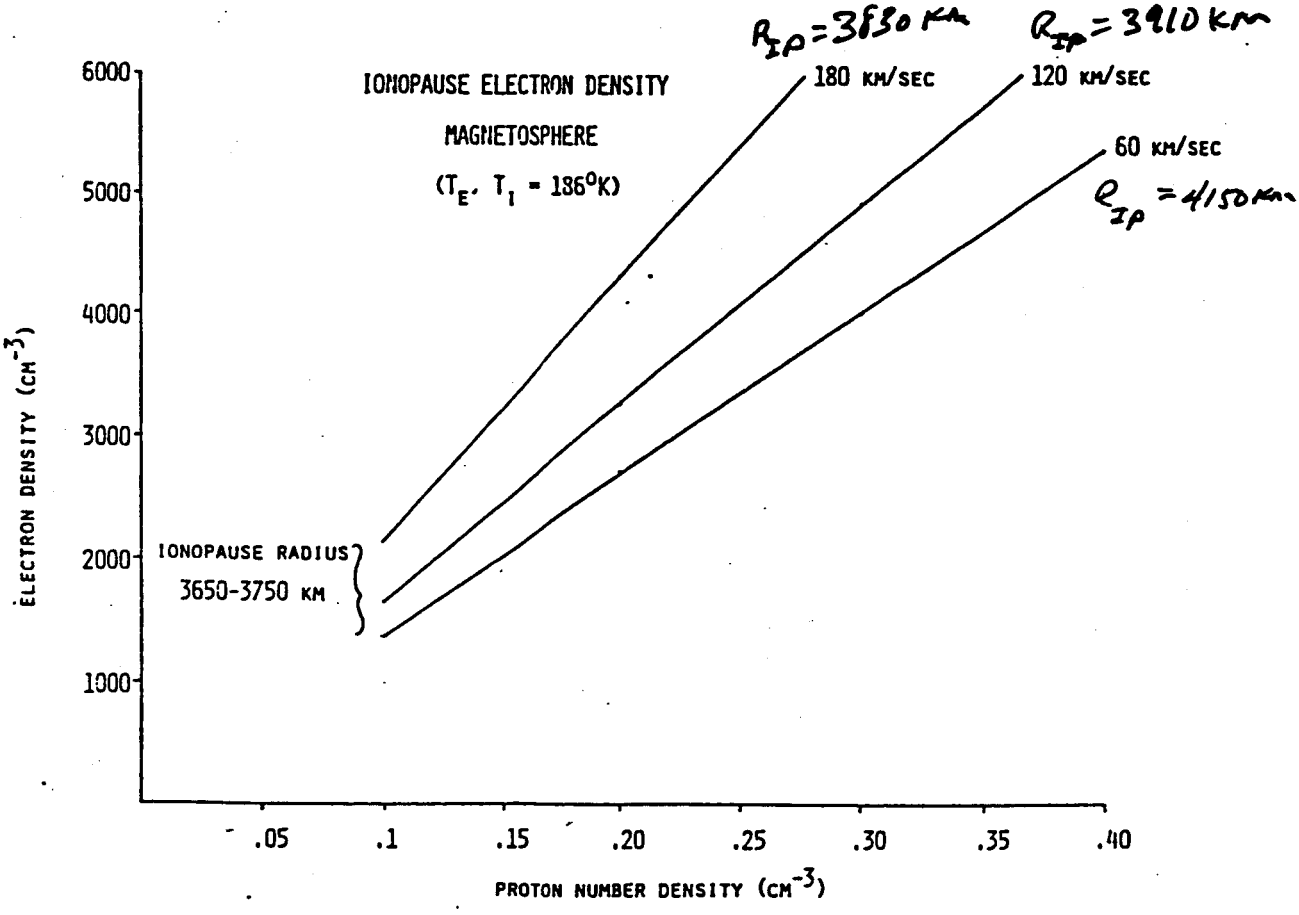

Figure 10b

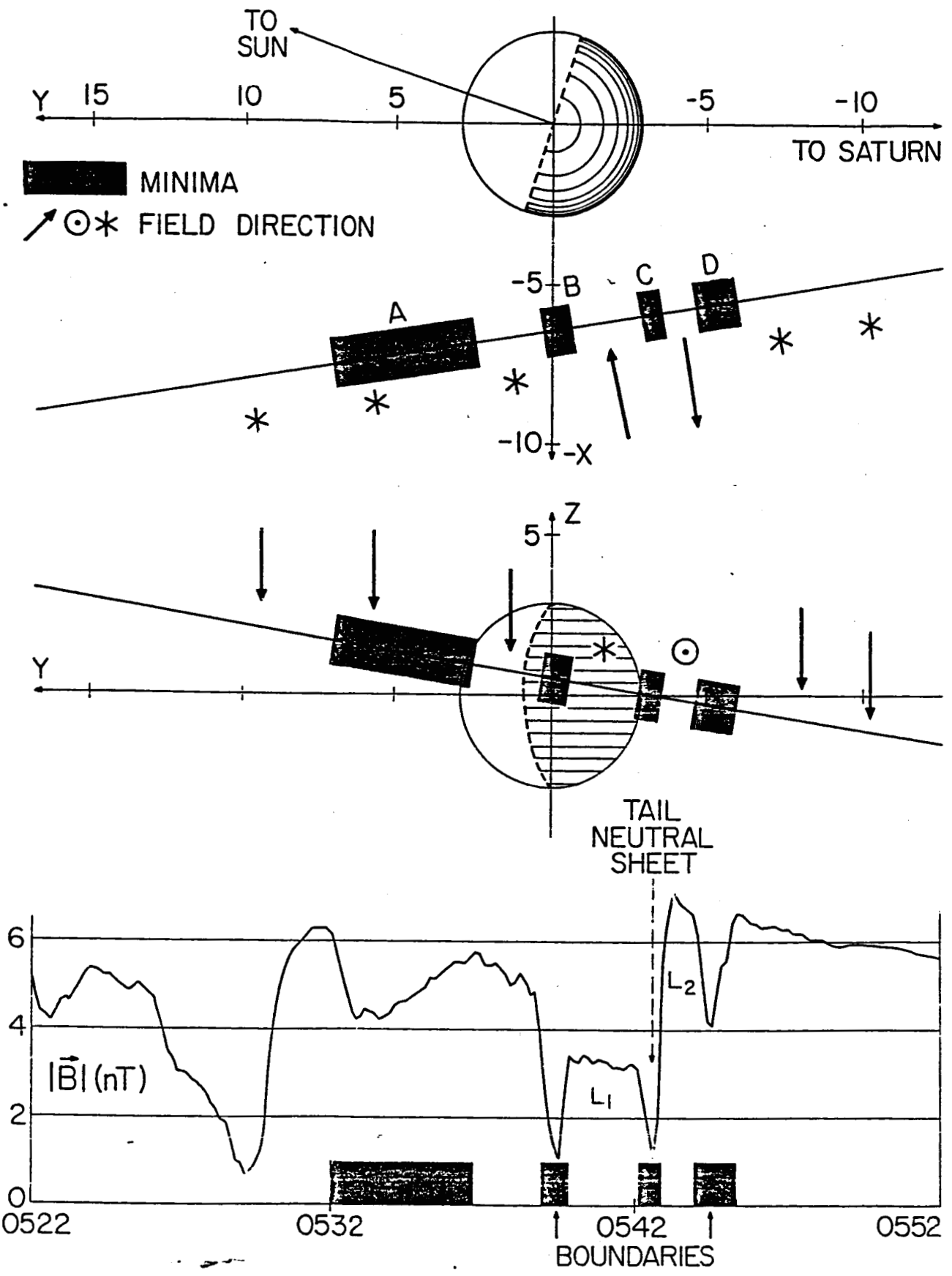
TO SUN
Y
15
10
5
-5
-10
TO SATURN
MINIMA
FIELD DIRECTION
A
B
C
D
-5
-10
-X
Z
5
Y
TAIL NEUTRAL SHEET
6
4
2
0
|B| (nT)
L1
L2
0522
0532
0542
0552
BOUNDARIES

Figure 11

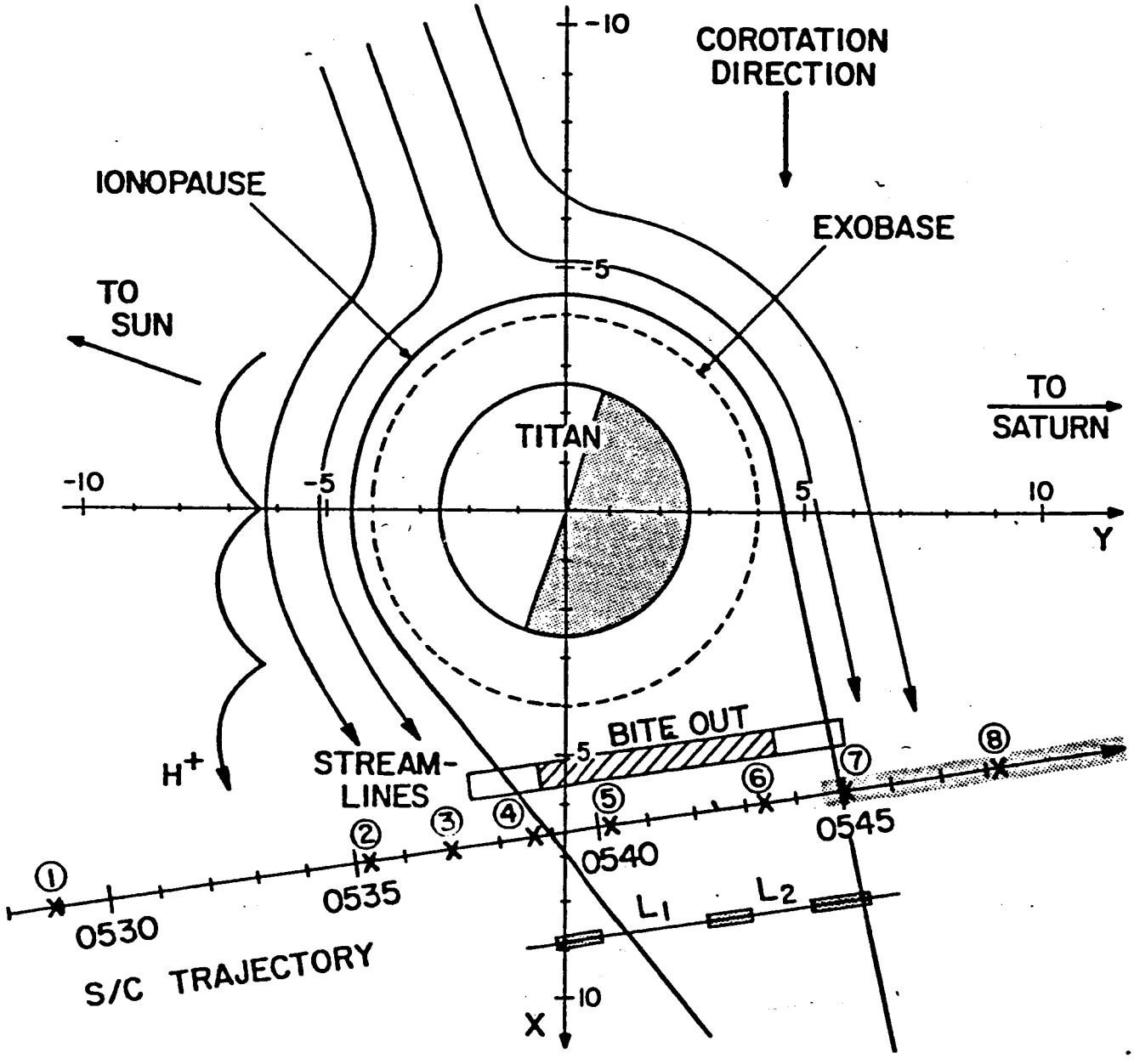

TITAN INTERACTION
NOV 12, 1980

Fig.12.

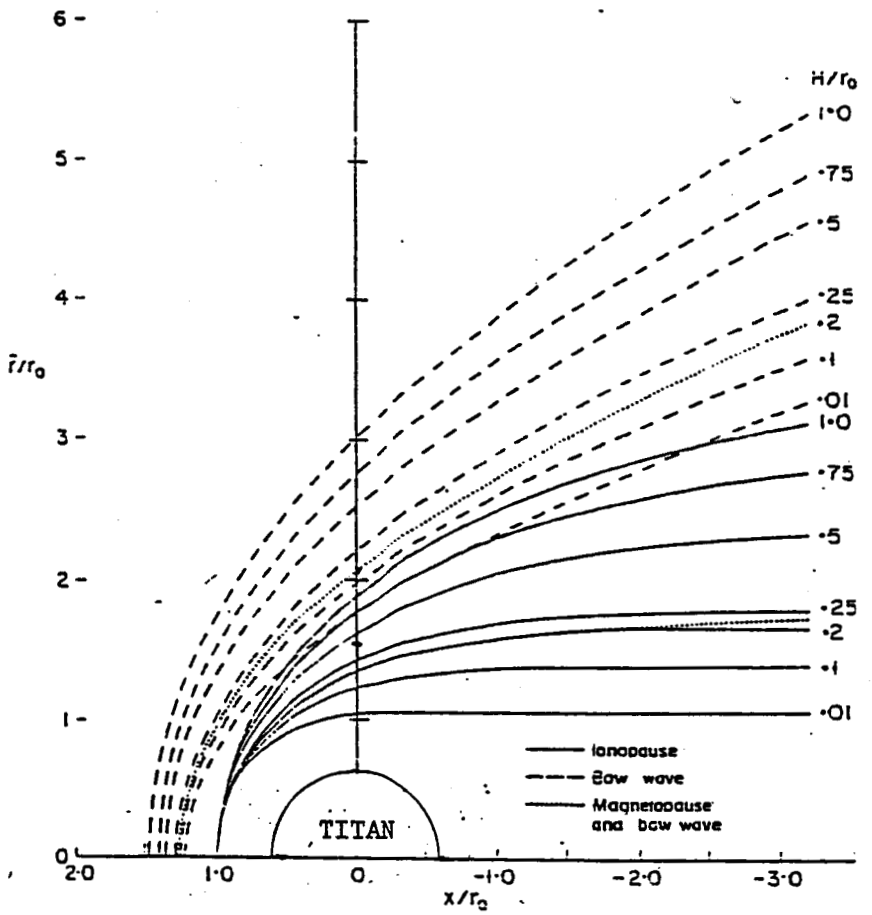

FIG. 4. CALCULATED LOCATION OF IONOPAUSE FOR VARIOUS H/r_0, AND ASSOCIATED LOCATION OF BOW WAVE FOR $M_\infty = 8, \gamma = \frac{4}{3}$.

Figure 13.

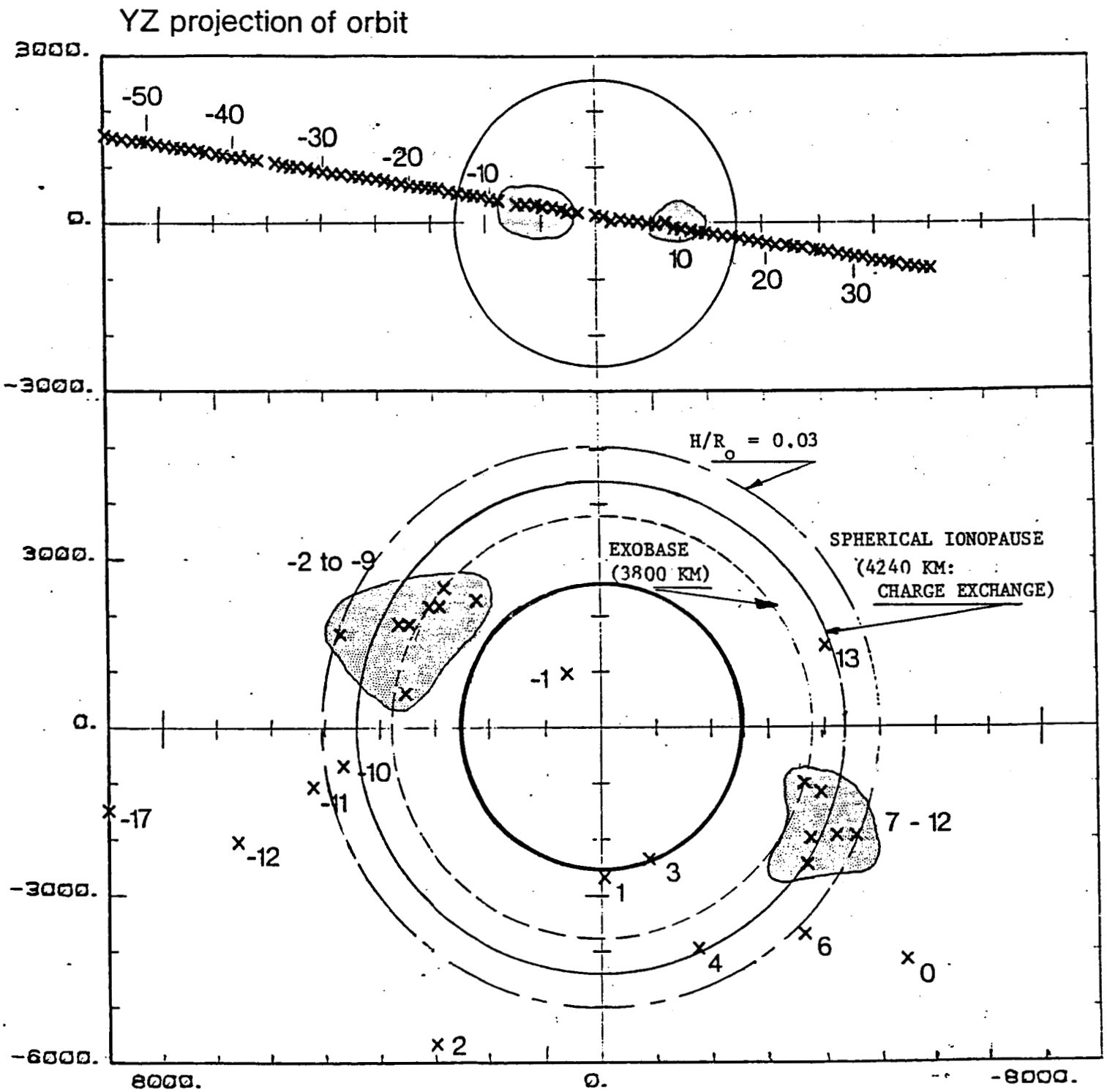

Figure 14

TITAN FLYBY: 27° ABERRATED COORDINATES

(KIVELSON AND RUSSELL, JGR 88, 49, 1983

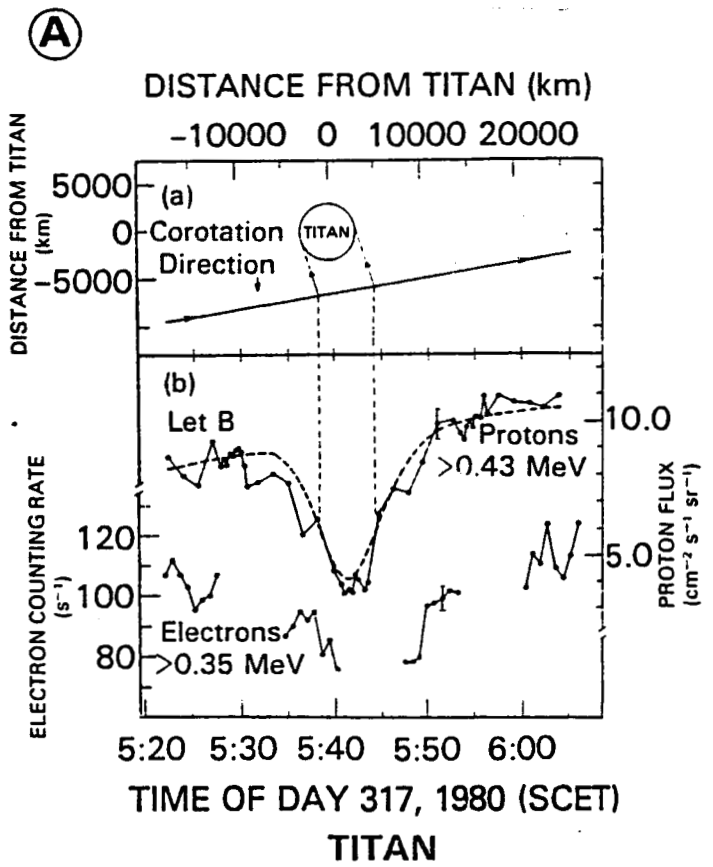

Figure 15a

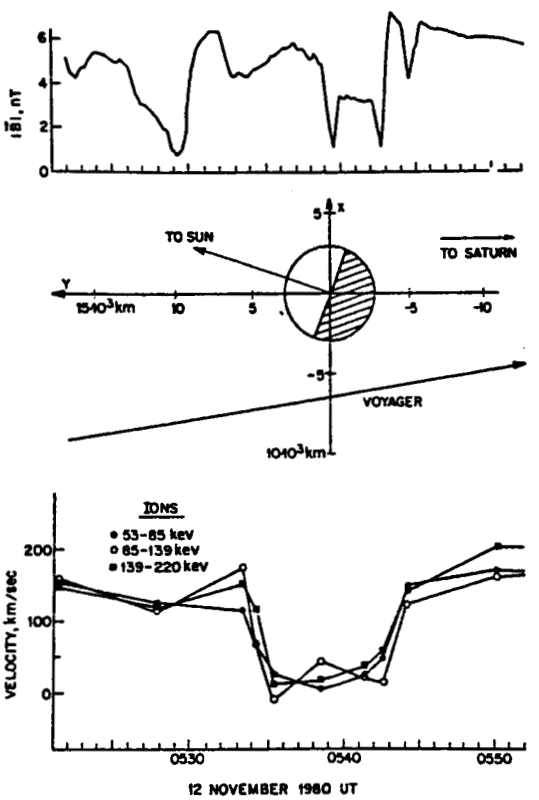

Figure 15b

TITAN'S BOW SHOCK

IN PERSPECTIVE

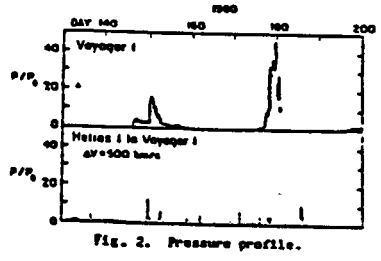

Fig. 2. Pressure profile.

(AFTER BURLAGA ET AL. 1983)

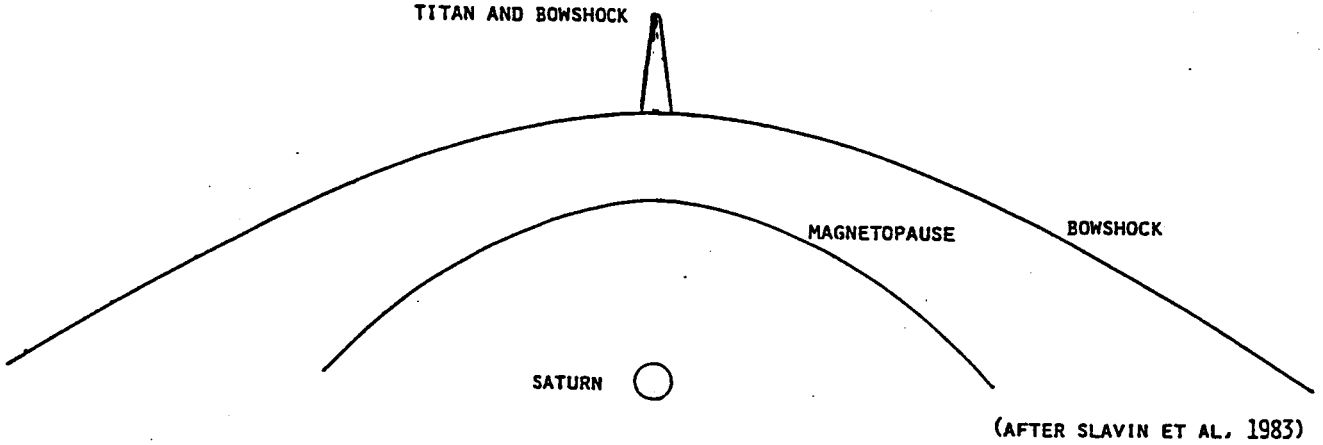

(AFTER SLAVIN ET AL. 1983)

Figure 16

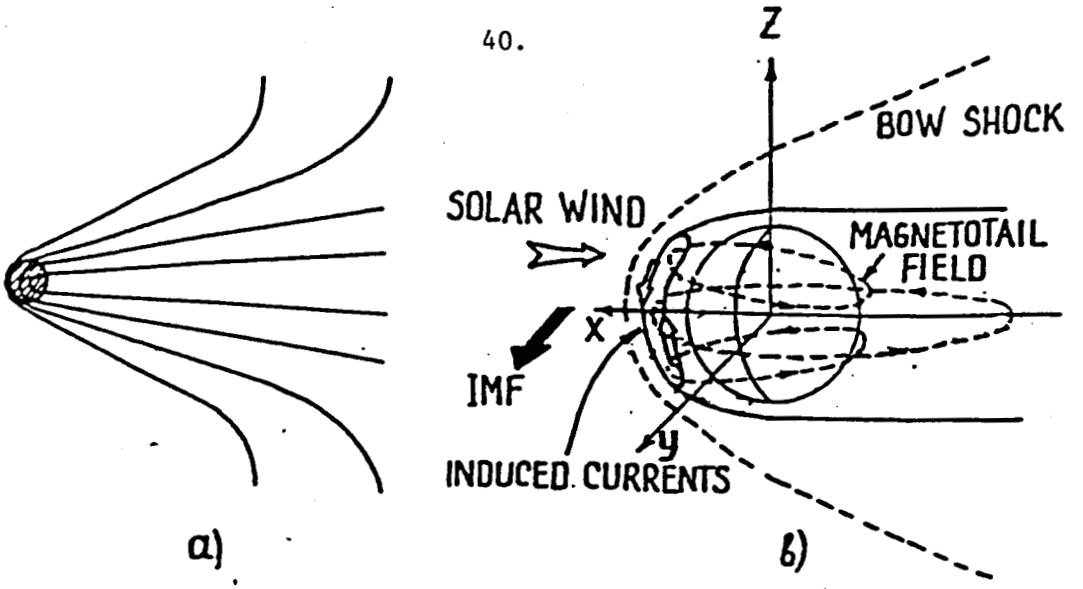

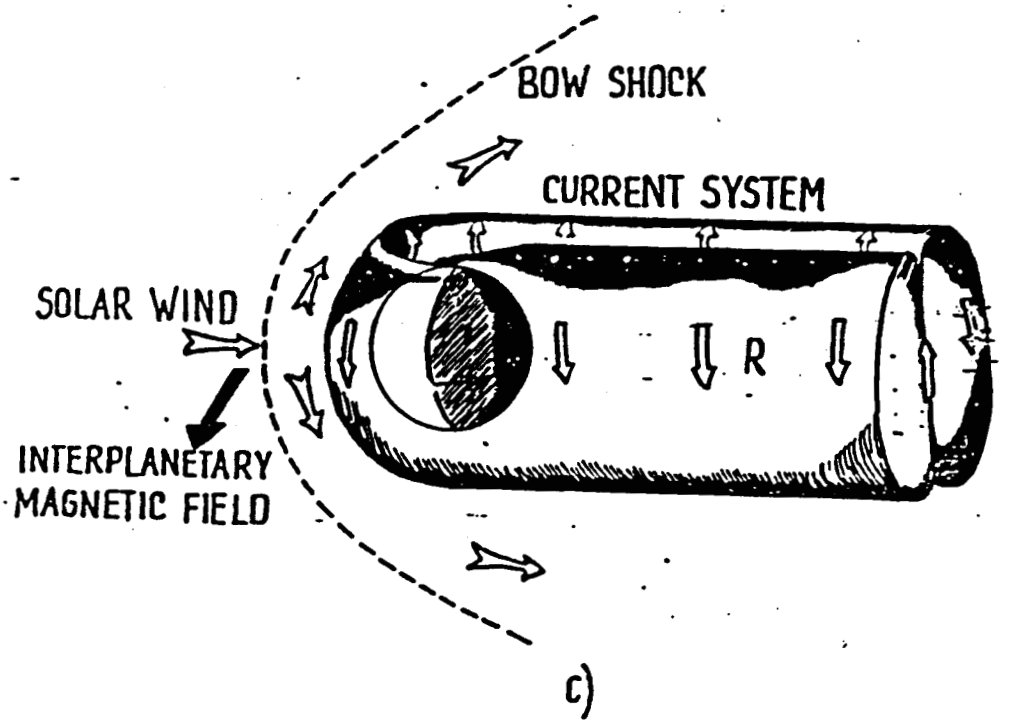

Figure 17

(Verigin, Gringauz, and Ness, 1983)

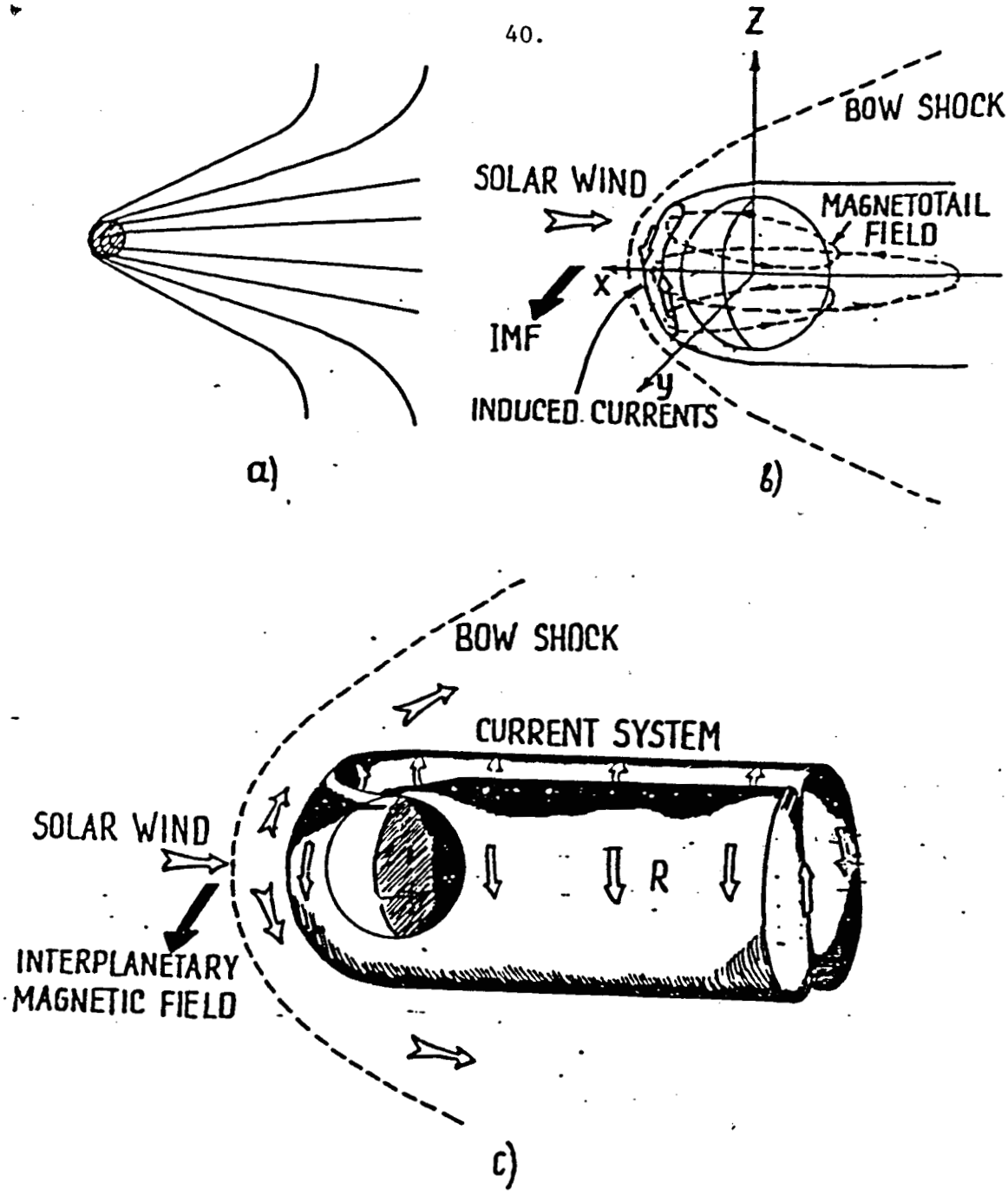

Figure 17

(Verigin, Gringauz, and Ness, 1983)

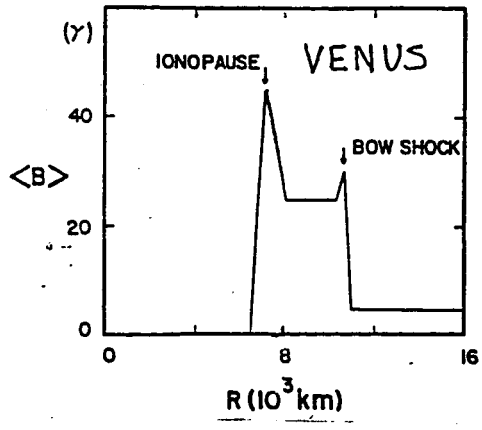

Figure 18a.

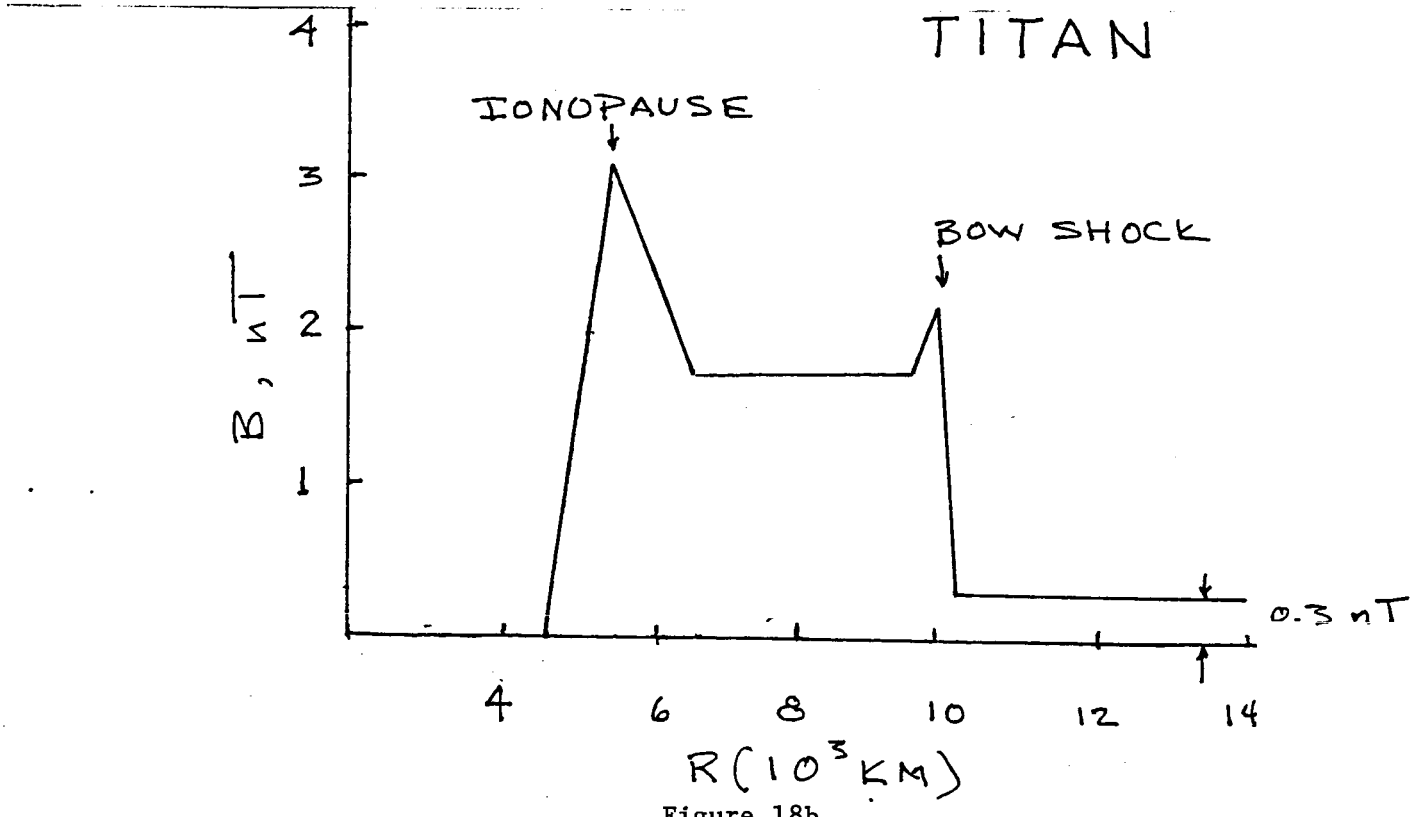

Figure 18b

* MASS LOADING AND CHARGE EXCHANGE NEGLECTED

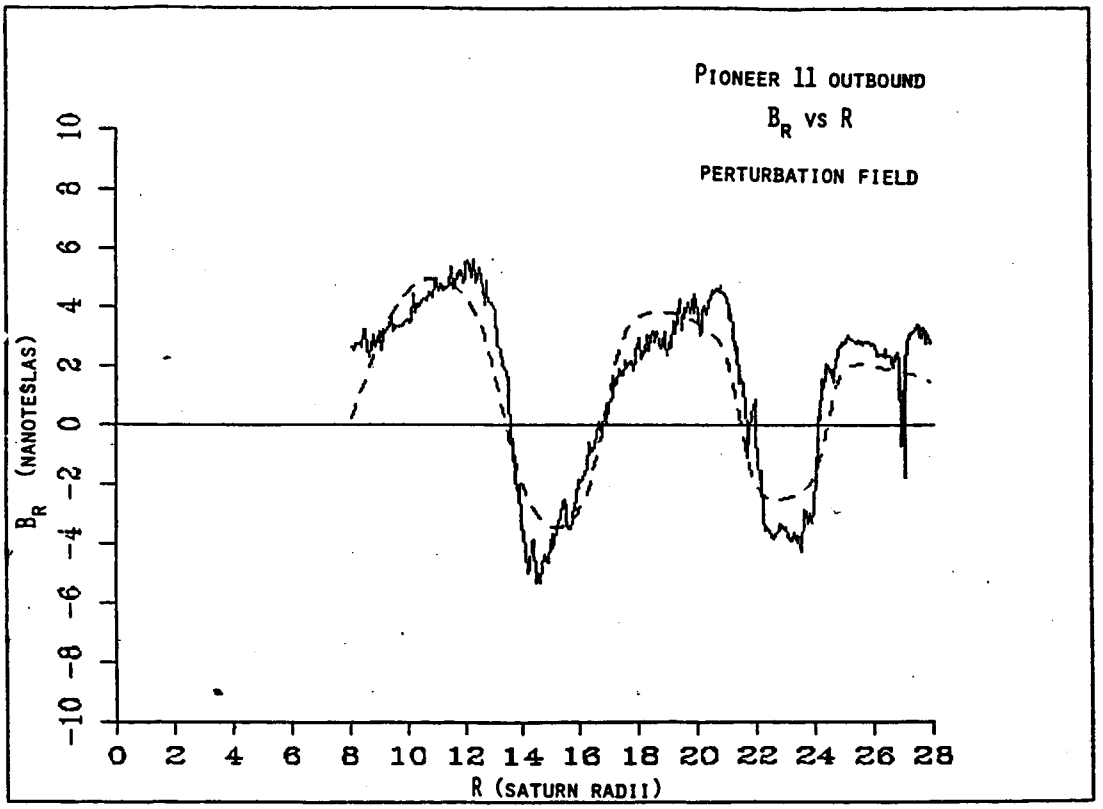

Figure 19a

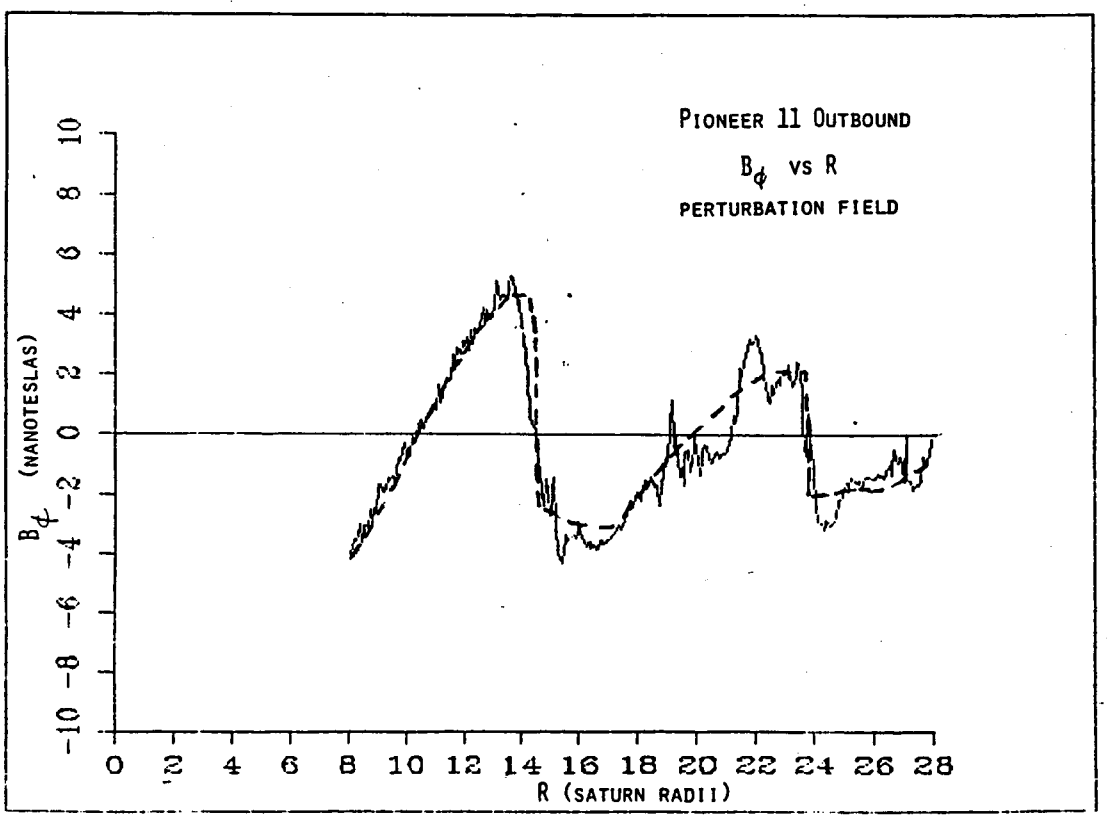

Figure 19b